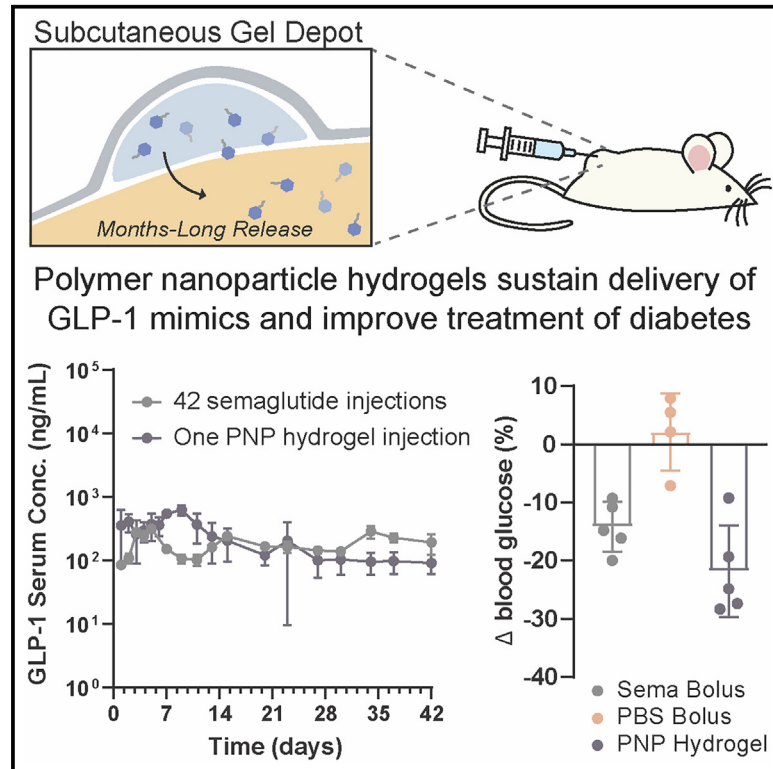


# Use of a biomimetic hydrogel depot technology for sustained delivery of GLP-1 receptor agonists reduces burden of diabetes management

## Graphical abstract



## Authors

Andrea I. d'Aquino, Caitlin L. Maikawa, Leslee T. Nguyen, ..., Hanne B. Andersen, Lotte Simonsen, Eric A. Appel

## Correspondence

eappel@stanford.edu

## In brief

d'Aquino et al. develop an injectable hydrogel depot technology enabling GLP-1 drugs potentially requiring administration only once every 4 months. The months-long-acting hydrogel-based drug products described here can dramatically reduce the frequency of therapeutic interventions, significantly increasing patient quality of life and reducing complications of diabetes management.

## Highlights

- Hydrogel depot technology enables a months-long GLP-1 drug product
- One shot maintains consistent exposure of GLP-1 receptor agonists over 42 days in rats
- Consistent, months-long drug exposure improves blood glucose and weight management



## Article

# Use of a biomimetic hydrogel depot technology for sustained delivery of GLP-1 receptor agonists reduces burden of diabetes management

Andrea I. d'Aquino,<sup>1</sup> Caitlin L. Maikawa,<sup>2</sup> Leslee T. Nguyen,<sup>3</sup> Katie Lu,<sup>4</sup> Ian A. Hall,<sup>2</sup> Carolyn K. Jons,<sup>1</sup> Catherine M. Kasse,<sup>1</sup> Jerry Yan,<sup>2</sup> Alexander N. Prossnitz,<sup>1</sup> Enmian Chang,<sup>1</sup> Sam W. Baker,<sup>5</sup> Lars Hovgaard,<sup>6</sup> Dorte B. Steensgaard,<sup>6</sup> Hanne B. Andersen,<sup>6</sup> Lotte Simonsen,<sup>7</sup> and Eric A. Appel<sup>1,2,8,9,10,11,\*</sup>

<sup>1</sup>Department of Materials Science & Engineering, Stanford University, Stanford, CA 94025, USA

<sup>2</sup>Department of Bioengineering, Stanford University, Stanford, CA 94305, USA

<sup>3</sup>Department of Biochemistry, Stanford University, Palo Alto, CA 94305, USA

<sup>4</sup>Department of Biology, Stanford University, Stanford, CA 94305, USA

<sup>5</sup>Department of Comparative Medicine, Stanford University, Palo Alto, CA 94305, USA

<sup>6</sup>Department of Biophysics and Formulations, Global Research Technologies, Novo Nordisk Park, 2760 Maaloev, Denmark

<sup>7</sup>Department of Obesity Research, Global Drug Discovery, Novo Nordisk Park, 2760 Maaloev, Denmark

<sup>8</sup>ChEM-H Institute, Stanford University, Stanford, CA 94305, USA

<sup>9</sup>Department of Pediatrics (Endocrinology), Stanford University, Stanford, CA 94305, USA

<sup>10</sup>Woods Institute for the Environment, Stanford University, Stanford, CA 94305, USA

<sup>11</sup>Lead contact

\*Correspondence: [eappel@stanford.edu](mailto:eappel@stanford.edu)

<https://doi.org/10.1016/j.xcrm.2023.101292>

## SUMMARY

Glucagon-like peptide-1 (GLP-1) is an incretin hormone and neurotransmitter secreted from intestinal L cells in response to nutrients to stimulate insulin and block glucagon secretion in a glucose-dependent manner. Long-acting GLP-1 receptor agonists (GLP-1 RAs) have become central to treating type 2 diabetes (T2D); however, these therapies are burdensome, as they must be taken daily or weekly. Technological innovations that enable less frequent administrations would reduce patient burden and increase patient compliance. Herein, we leverage an injectable hydrogel depot technology to develop a GLP-1 RA drug product capable of months-long GLP-1 RA delivery. Using a rat model of T2D, we confirm that one injection of hydrogel-based therapy sustains exposure of GLP-1 RA over 42 days, corresponding to a once-every-4-months therapy in humans. Hydrogel therapy maintains management of blood glucose and weight comparable to daily injections of a leading GLP-1 RA drug. This long-acting GLP-1 RA treatment is a promising therapy for more effective T2D management.

## INTRODUCTION

Of almost 500 million people living with diabetes or prediabetes worldwide, an estimated 130 million live in the United States.<sup>1,2</sup> In the United States alone, the annual spending directly related to diabetes and pre-diabetes amounts to roughly \$400 billion. This makes it the tenth most costly disease in the United States.<sup>1,3</sup> Type 2 diabetes (T2D), which accounts for 90%–95% of all diabetes cases, is a metabolic disorder characterized by insulin resistance, deterioration of pancreatic  $\beta$  cell function, and impaired regulation of hepatic glucose production eventually leading to  $\beta$  cell failure.<sup>4–6</sup> Patients with poorly managed T2D are at risk of serious micro- and macrovascular complications, including cardiovascular disease, nephropathy, retinopathy, neuropathy, and stroke. In addition to insufficient access to care, poor adherence to treatment is a general problem.<sup>7,8</sup> The lack of adherence occurs primarily because of adverse effects, most commonly being hypoglycemia, weight gain, or

gastrointestinal side effects, and complex treatment regimens.<sup>7,8</sup> Treatment strategies that alleviate patient burden while providing optimal glycemic control would transform the treatment of T2D and improve patient outcomes.

Glucagon-like peptide-1 receptor agonists (GLP-1 RAs) have become central to the treatment of T2D due to their beneficial effects that extend beyond improving glucose control.<sup>9,10</sup> GLP-1 is an incretin hormone secreted from intestinal L cells in response to nutrients that lowers blood glucose by stimulating insulin and suppressing glucagon secretion in a glucose-dependent manner, reducing the risk of hypoglycemia.<sup>11</sup> In addition, GLP-1 is also a neurotransmitter synthesized by preproglucagon neurons in the brain and acts via central pathways to lower energy intake through an effect on satiety, hunger, and reward-related measures,<sup>12,13</sup> leading to a lowering of body weight, which has prompted the approval of liraglutide and semaglutide for the treatment of obesity.<sup>14–18</sup> Importantly, liraglutide is currently the only GLP-1 RA that is FDA approved for use in children ages 12–17 years



with obesity.<sup>19</sup> Long-acting GLP-1 RAs also reduce risk of cardiovascular disease,<sup>20–22</sup> making them attractive treatment options for people who are at increased risk of these disorders. Importantly, it has been established that the optimal therapeutic effect of GLP-1 is achieved with regimens that provide sustained plasma levels of active peptide.<sup>9–11</sup> Such regimens include continuous subcutaneous infusion of GLP-1<sup>12–14</sup> and once- or twice-daily or weekly injections of GLP-1 analogs with extended plasma stability.<sup>14,15</sup> Improved delivery technologies that provide sustained plasma levels of GLP-1 RAs are important for treating diabetes.

Several strategies have been employed for stabilizing GLP-1 RAs and prolonging therapeutic efficacy, resulting in the development of T2D drug products with treatment regimens ranging from twice daily to once weekly.<sup>10</sup> Liraglutide and semaglutide are based on the native GLP-1 sequence and carry a single fatty acid and linker modification enabling reversible binding to albumin to extend the circulating half-life while maintaining optimal potency. While liraglutide has a pharmacokinetic profile supporting once-daily dosing, semaglutide has extended pharmacokinetics and once-weekly dosing enabled by further improved metabolic stability and a dicarboxylic fatty acid side chain facilitating a stronger binding to albumin.<sup>23</sup> While reducing treatment frequency from daily to weekly is associated with improved patient adherence, there is still room for improvement to reduce treatment burden and improve patient compliance (Figure 1A).<sup>24–26</sup> To address this challenge, we sought to develop long-acting formulations of semaglutide and liraglutide that provide continuous therapy for upward of 4 months from a single administration to coincide with the typical cadence with which T2D patients visit their endocrinologist or primary care provider (Figures 1B and 1C).<sup>27</sup>

In this work, we drew inspiration from long-acting drug products such as Lupron Depot, containing leuporelin, which is an effective microparticle-based leuporelin formulation for treatment of endometriosis developed for administration once every 3 months.<sup>28</sup> In addition, 1-, 3-, 4- and 6-month microparticle-based leuporelin depot formulations are widely used for treatment of advanced and metastatic prostate cancer.<sup>29</sup> Similarly, exenatide is commercially available in a microparticle-based extended-release formulation enabling once-weekly administration.<sup>64</sup> While these microparticle-based drug-delivery technologies have significantly improved the utility of exenatide as a pharmaceutical agent by enabling once-weekly dosing, they have unfortunately required significant optimization to achieve appropriate drug-depot compatibility and release behavior, and only relatively hydrophobic peptides have demonstrated months-long release.<sup>30</sup> For this reason, we sought to engineer an injectable hydrogel depot technology capable of months-long release of GLP-1 RAs. Hydrogels address some of the shortcomings of microparticle technologies, as they maintain the native aqueous environment around the encapsulated drugs and are therefore compatible with existing approved drug molecules developed for aqueous formulation. While many hydrogel-based depot technologies have been reported in the literature to show attractive local tolerance,<sup>31</sup> they typically exhibit several critical shortcomings, including: (1) complicated manufacturing and poor formulation stability, (2) challenging administration, (3) burst release that can contribute to poor tolerability of the therapy,

and (4) insufficiently slow release to enable appropriately long-acting therapies. We therefore sought to leverage an injectable hydrogel platform generated through self-assembly of dynamic, entropically driven supramolecular interactions between biodegradable nanoparticles (NPs) and hydrophobically modified hydroxypropyl methylcellulose (HPMC) derivatives to develop a long-acting GLP-1 RA formulation (Figure 1E).<sup>32–39</sup> We have previously shown these polymer-NP (PNP) hydrogels to be capable of providing application-specific release of diverse biopharmaceuticals, such as proteins, vaccines, and cells, that is tunable over time frames extending from days to upward of 6 months.<sup>33,37,40–44</sup>

Unlike traditional covalently cross-linked hydrogels, PNP hydrogels are formed through strong yet dynamic physical interactions. As a result, these materials address the shortcomings of other hydrogel-based depot technologies, as they exhibit: (1) mild formulation requirements favorable for maintaining drug stability during manufacturing and storage, (2) pronounced shear thinning properties enabling injection through clinically relevant needles, (3) rapid self-healing of hydrogel structure and depot formation mitigating burst release of the drug cargo, (4) sufficiently high-yield stress to form a robust depot that persists under the normal stresses of the subcutaneous space following administration, and (5) prolonged delivery of therapeutic cargo.<sup>45</sup> These hydrogels are by design biodegradable and have been shown to be non-immunogenic in mice, rats, pigs, and sheep, as well as not promoting immune responses to their payloads.<sup>33–39,41,44</sup> Moreover, these gels can be formulated and stored in prefilled syringes and maintain stability under standard storage conditions.<sup>39</sup> Herein, we sought to optimize GLP-1 RA pharmacokinetics by engineering the drug encapsulation and release characteristics of these PNP hydrogels, enabling the development of a months-long-acting GLP-1 RA drug product capable of reducing treatment burden to more effectively manage T2D.

## RESULTS

### Development of injectable hydrogels for sustained release of GLP-1 RAs

Liraglutide and semaglutide were considered excellent therapeutic cargo for sustained delivery from PNP hydrogel depot materials due to the hydrophobic fatty acid modifications.<sup>23,46,47</sup> We hypothesized that these fatty acid moieties could non-covalently embed the biopharmaceutical within the hydrogel network with simple mixing during hydrogel fabrication (Figure 1D). This embedding is made possible by the fact that the poly(lactic acid) core of the poly(ethylene glycol)-*b*-poly(lactic acid) (PEG-PLA) NPs within the hydrogel structure is hydrophobic in nature and the HPMC-C<sub>12</sub> polymers possess hydrophobic moieties, both of which act as sites for non-covalent, hydrophobic interactions between the drug molecules and the hydrogel components. As the standard clinical dosing of semaglutide for T2D is ~1 mg weekly, we anticipated that a single administration capable of providing upward of 4 months of continuous therapy must contain ~20 mg of semaglutide in a volume relevant for subcutaneous administration (e.g., generally 0.5–2 mL). We have previously reported that these injectable, biocompatible PNP hydrogel materials are capable of facile loading of diverse

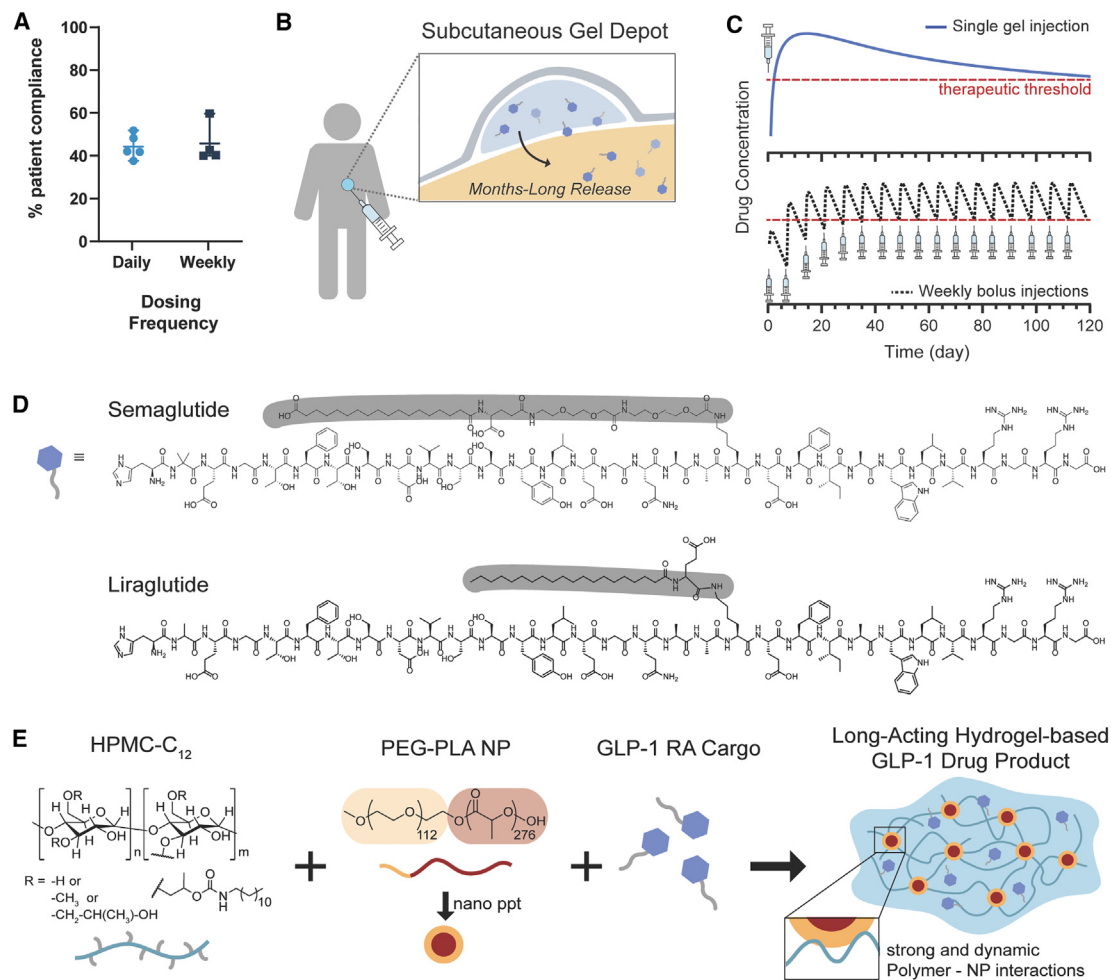


**Figure 1. PNP hydrogels for the prolonged delivery of GLP-1 RAs**

(A) From literature reports it is clear that once-weekly dosing frequency does not significantly improve patient compliance compared with a once-daily dosing frequency.<sup>7</sup>

(B) Localized depots form in the subcutaneous space immediately after subcutaneous injection, providing a tunable platform for sustained release of GLP-1-RA compounds.

(C) Clinical data showing the release profile of current GLP-1 treatments, where the black dotted line represents repeated weekly injections that patients take every week for 4 months to reach therapeutic concentrations of GLP-1 RA. In contrast, the blue line represents the target delivery profile of a single PNP hydrogel depot injection that sustains release of GLP-1 RA for 120 days. Current state-of-the-art strategies require daily or weekly subcutaneous injections with significant ramp-up time to achieve therapeutic concentrations. The red dotted line indicates the therapeutic threshold.

(D) Semaglutide and liraglutide are once-weekly and once-daily, respectively, GLP-1 RA therapies that were investigated in this study.

(E) PNP hydrogels prepared by mixing hydrophobically modified HPMC with PEG-PLA nanoparticles enable facile encapsulation of GLP-1-receptor agonists with 100% efficiency.

protein cargo at relevant concentrations with high efficiency and enable tunable cargo delivery time frames.<sup>33,37,40–44</sup>

PNP hydrogels are fabricated by mixing a solution of dodecyl-modified HPMC (HPMC-C<sub>12</sub>) with a solution of biodegradable NPs composed of PEG-PLA, comprising the pharmaceutical agent of interest (Figure 1).<sup>37</sup> To form these hydrogels, a solution of PEG-PLA NPs is loaded into one sterile syringe, while a solution of HPMC-C<sub>12</sub> is loaded into a separate syringe, and the two solutions are mixed with a sterile Luer lock elbow mixer (Figure 2A). Upon mixing, the strong yet dynamic PNP interactions between the HPMC-C<sub>12</sub> polymers and the PEG-PLA NPs constitute physical cross-linking that drives formation of a solid-like hy-

drogel material with 100% loading efficiency of the pharmaceutical agent (Figure 2A). The properties of these PNP hydrogels can be tuned through alteration of the formulation (i.e., the concentration of HPMC-C<sub>12</sub> and PEG-PLA NPs), enabling facile modulation of the rates of hydrogel erosion and commensurate payload release. We have previously reported that these hydrogels are exceptionally well tolerated in numerous indications and do not exhibit swelling when exposed to physiologic conditions.<sup>34,48</sup> These PNP hydrogels, therefore, can be readily optimized to target desirable release characteristics for pharmaceutical agents of interest in a broad range of therapeutic applications.

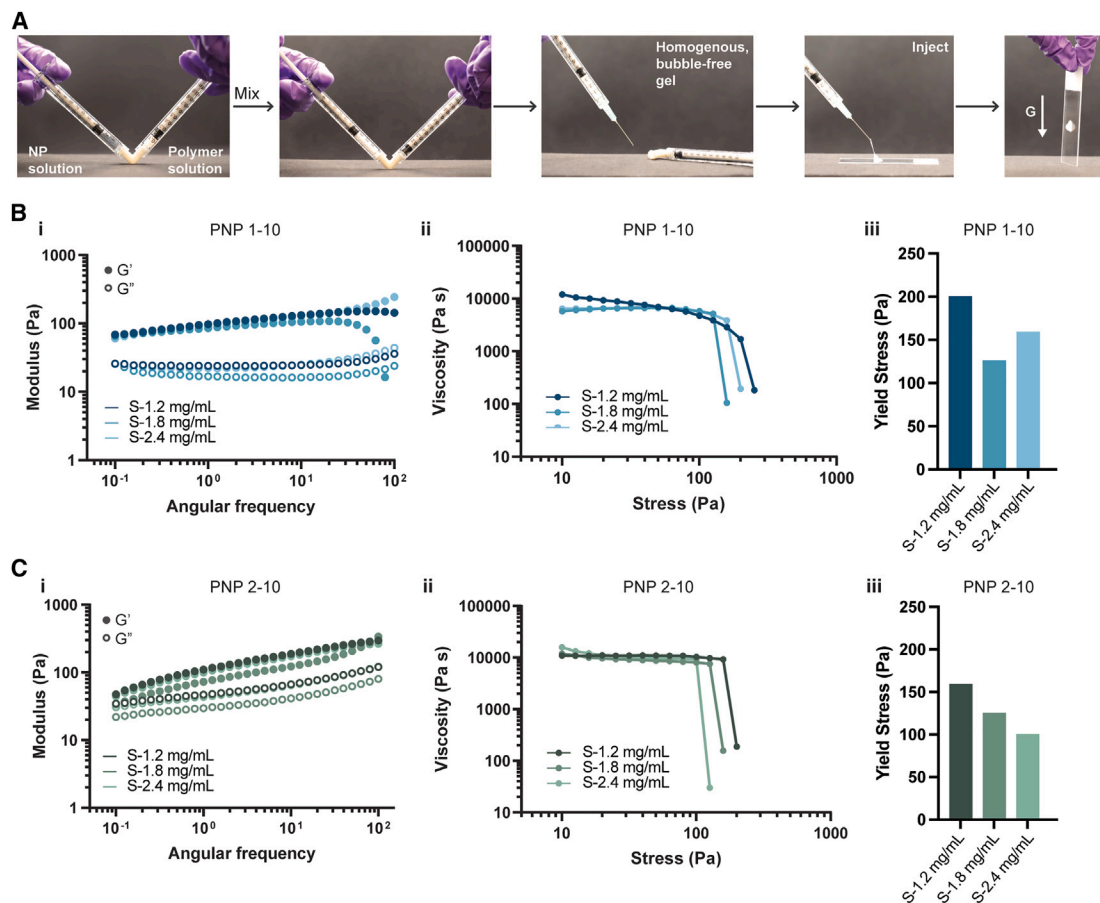


**Figure 2. Preparation and characterization of GLP-1 RA-loaded PNP hydrogel formulations**

(A) PNP hydrogels are prepared by mixing a solution of hydrophobically modified HPMC (right syringe) with a solution of PEG-PLA nanoparticles and GLP-1 RAs (left syringe) using a Luer lock mixer. After mixing, a homogeneous, bubble-free, solid-like PNP hydrogel is formed (right syringe). Owing to their dynamic cross-linking, PNP hydrogels are injectable through clinically relevant, high-gauge needles and rapidly self-heal after injection.

(B) Rheological characterization of PNP-1-10 hydrogel formulations: (i) frequency-dependent oscillatory shear sweep, (ii) stress-dependent oscillatory shear sweep, and (iii) yield stress obtained from stress sweep.

(C) Rheological characterization of PNP-2-10 hydrogel formulations: (i) frequency-dependent oscillatory shear sweep, (ii) stress-dependent oscillatory shear sweep, and (iii) yield stress obtained from stress sweep.

### Rheological characterization of GLP-1 RA-loaded PNP hydrogels

We prepared two PNP hydrogel formulations, PNP-1-10 and PNP-2-10, where the first number denotes the weight percent (wt %) of the polymer and the second number denotes the wt % of the NPs (n.b., the remaining mass is buffer). For all *in vitro* studies, PNP hydrogel formulations comprising semaglutide were denoted with an “S” followed by their corresponding drug loading (e.g., S-1.8 mg/mL), while liraglutide formulations were denoted with an “L” followed by their corresponding drug loading (e.g., L-1.8 mg/mL). For all *in vivo* results, PNP hydrogel formulations comprising semaglutide were denoted with an “S” followed by their corresponding dosage (e.g., S-0.9 mg), while liraglutide formulations were denoted with an “L” followed by their corresponding dosage (e.g., L-0.9 mg). We targeted a GLP-1-RA concentration and dosage relevant to human-equivalent dosing of semaglutide (clinical dosing of semaglutide is  $\sim 1$  mg weekly)<sup>49,50</sup> for evaluation in a rat model of in-

sulin-impaired diabetes. Despite the higher dose of liraglutide required for clinically relevant effect in T2D (1.8 mg/day for liraglutide compared with 1 mg/week for semaglutide), we formulated materials with equal doses of liraglutide and semaglutide to make mechanistic comparisons on incorporation and release of the peptides from the PNP hydrogels.

The rheological properties of PNP hydrogels with different loadings of both liraglutide and semaglutide were evaluated to ensure that the cargo loading did not alter the hydrogel properties integral for injectability, depot formation, and depot persistence (Figures 2B, 2C, and S1). Frequency-dependent oscillatory shear rheological testing showed that PNP hydrogel formulations exhibit solid-like behavior ( $G' > G''$ ;  $\tan(\delta) = 0.1\text{--}0.5$ ) across the entire range of frequencies evaluated within the linear viscoelastic regime of these materials, meaning that all PNP hydrogel formulations demonstrate mechanical properties essential for depot formation (Figures 2Bi and 2Ci). Moreover, the stiffness ( $G'$ ) of these materials increased with higher



polymer content. Stress-controlled oscillatory shear measurements were used to evaluate yield stress and flow behavior of these materials (Figures 2Bii/iii and 2Cii/iii). Only slight differences in yield stress values were observed between the 1-10 and the 2-10 formulations, whereby yield stress increased with increasing polymer content and negligibly lowered with the incorporation of either liraglutide or semaglutide drug molecules. At stresses below their yield stress, these materials do not flow; however, when the stress exceeds their yield stress, the materials flow and the observed viscosity drops dramatically (Figures 2B and 2C). In addition, all PNP hydrogel formulations displayed shear-thinning behavior without fracture with increasing shear rates. The high degree of shear-thinning and rapid self-healing behavior observed for these PNP hydrogels loaded with GLP-1 RAs not only enables injection through clinically relevant, small-diameter needles,<sup>45</sup> but also prevents significant burst release immediately after injection on account of rapid depot formation in the body.<sup>33,43,44</sup> Furthermore, the yield stress behavior exhibited by these materials ( $\tau_y > 100$  Pa) is crucial for formation of persistent depots in the subcutaneous space upon administration.<sup>48</sup>

#### **In vitro release kinetics of GLP-1 RAs from PNP hydrogel formulations**

Next, we investigated the release behaviors of semaglutide and liraglutide from PNP hydrogel formulations *in vitro*. To study these behaviors, drug-loaded hydrogels were loaded into capillaries by injection and PBS was added to mimic infinite sink conditions at physiological temperature. Aliquots of the surrounding medium were taken and the concentration of either semaglutide or liraglutide was quantified by ELISA to measure the release kinetics of each drug from the hydrogel formulations over time (Figure 3A; Method S1). At the end of the study, the remaining hydrogel was dissolved and the retained cargo quantified by ELISA.

We compared the release of semaglutide (S-1.8 mg/mL) and liraglutide (L-1.8 mg/mL) from both PNP-1-10 and PNP-2-10 hydrogel formulations over the course of 2 weeks. For semaglutide in either hydrogel formulation, a clear plateau in cargo release was reached after the first week of the study, whereas liraglutide exhibited negligible release throughout the study, indicative of a zero-order release profile. For semaglutide formulations, the PNP-1-10 formulation released  $50\% \pm 5\%$  of the entrapped cargo over the 2-week study, while the PNP-2-10 formulation released  $54\% \pm 6\%$  of cargo over the same time frame (Figure 3B). In contrast, PNP-1-10 and PNP-2-10 hydrogel formulations comprising liraglutide released only  $0.4\% \pm 0.2\%$  and  $0.2\% \pm 0.04\%$  of their cargo, respectively, over the course of the 2-week study (Figure 3C). From these studies, we observed that only approximately 50% of the semaglutide was retained in these hydrogels, while nearly 100% of the liraglutide was retained over prolonged time frames in this release format where hydrogel erosion is negligible over time (Figure 3D;  $p < 0.001$  for comparison of semaglutide and liraglutide release).

Gastrointestinal adverse effects are common with GLP-1 RA therapy and are related to abrupt increases in drug plasma levels, which are clinically mitigated by gradual up-titration. Thus, we sought to evaluate the burst release of these cargoes

from the PNP hydrogels, which may lead to undesirable high drug exposure. We established an assay in which we injected drug-loaded hydrogels directly into PBS to recapitulate the process of transcutaneous injection into the subcutaneous space and investigated the level of burst release within the first minute after injection. The amount of released drug was quantified by ELISA 1 min after injection (Figure 3E). In this assay, the S-1.8 mg/mL 2-10 formulation released  $1.4\% \pm 0.09\%$  of cargo, while the S-1.8 mg/mL 1-10 formulation released  $1.6\% \pm 0.08\%$  of cargo. In contrast, liraglutide formulations displayed significantly less burst release, with the L-1.8 mg/mL 2-10 formulation releasing  $0.3\% \pm 0.4\%$  of cargo and the L-1.8 mg/mL 1-10 formulation releasing  $0.7\% \pm 0.1\%$  of cargo. Similar to the *in vitro* release studies (Figures 3B–3D), the semaglutide-loaded hydrogels showed a significantly greater initial burst release compared with liraglutide-loaded hydrogels ( $p < 0.001$  for comparison of semaglutide and liraglutide release).

As we see a higher amount of burst release and lower proportion of drug retained over prolonged time frames for semaglutide, we hypothesized that there is likely a substantial fraction of “free” cargo (i.e., not adhered to the PNP hydrogel matrix) that undergoes fast, diffusion-based release. Such “free” drug would be expected to be subject to diffusional release over time, whereas “bound” drug would be released only by hydrogel erosion,<sup>51</sup> which is severely limited in this capillary release model (Figure 3F). In contrast, liraglutide exhibited significantly higher retention within the PNP hydrogels compared with semaglutide ( $p = 0.0003$ ; L-1.8 mg/mL 1-10 vs. S-1.8 mg/mL 1-10 formulation). As liraglutide formulations exhibited almost complete cargo retention and negligible burst release, we hypothesize that essentially all of the cargo is adhered to the PNP hydrogel structure and will undergo slow erosion-based release (Figure 3F). While liraglutide contains a C<sub>12</sub> linker with a single carboxylic acid, semaglutide contains a C<sub>18</sub> linker with two carboxylic acid moieties, making it significantly more hydrophilic.<sup>23</sup> These physicochemical differences may explain the observed differences in interaction and resulting release behavior of the drugs with the hydrophobic interface of the PEG-PLA NPs of the PNP hydrogels.

#### **In vivo pharmacokinetics of hydrogel-based GLP-1 RA formulations**

Prolonged delivery of GLP-1 RAs affords the opportunity for a months-long-acting T2D therapy that provides steady levels of the incretin hormone to reduce the burden of maintaining glucose homeostasis. To assess the performance of our hydrogel-based formulations *in vivo*, we conducted pharmacokinetic and pharmacodynamic studies in a rat model of insulin-impaired diabetes (Figure 4). Diabetes was induced using a combination of streptozotocin (STZ) and nicotinamide (NA) in rats, which is a mimic of a T2D-like phenotype (Method S2).<sup>52,53</sup>

Following the onset of diabetes according to literature procedures,<sup>53,54</sup> rats were fasted overnight to ensure an average starting blood glucose (BG) level of approximately 130–200 mg/dL.<sup>55</sup> Fasting BG levels were then measured once a day for 5 days before treatment and rats were considered diabetic when at least three of five fasting BG measurements, taken over the course of 5 days, fell between 130 and 200 mg/dL. Animals

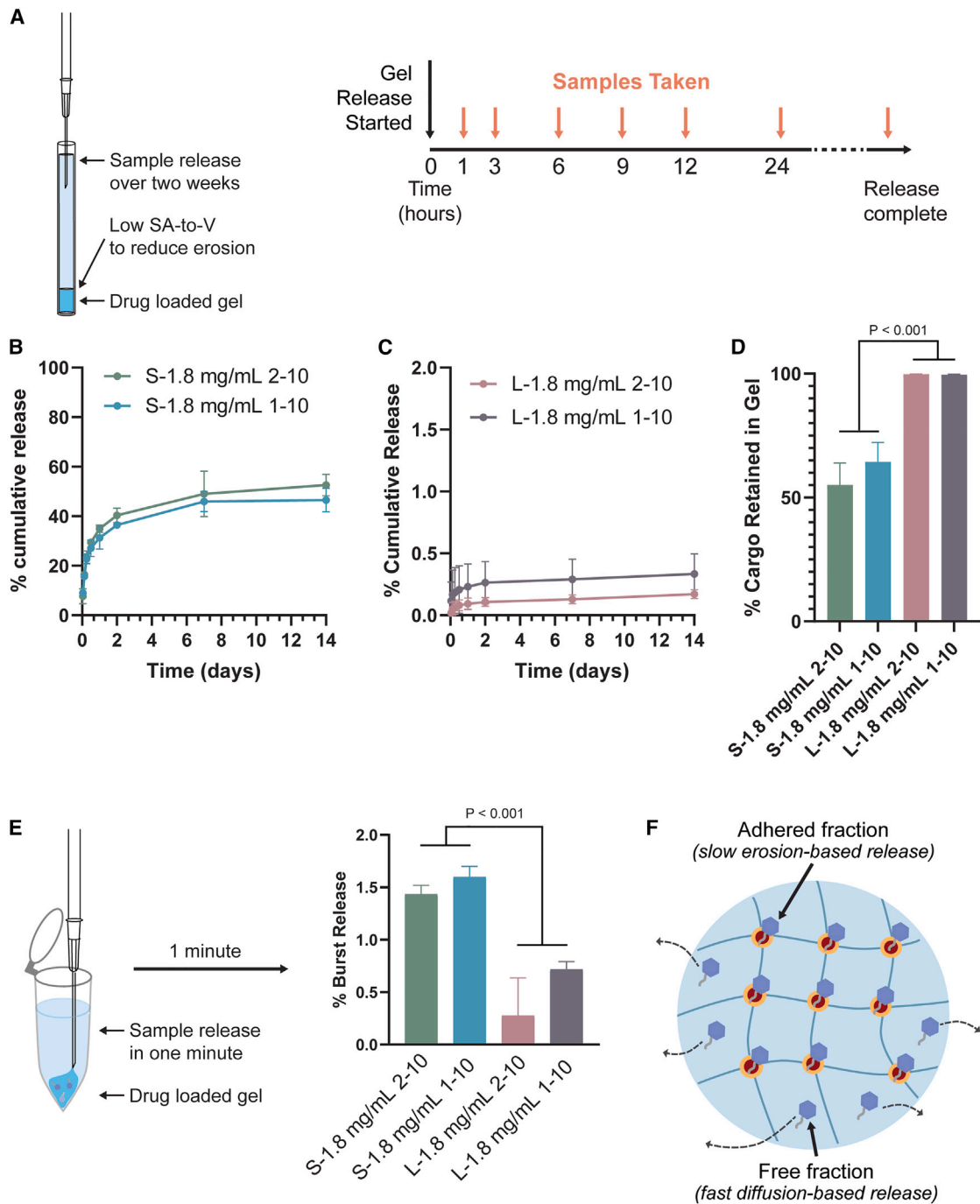


**Figure 3. *In vitro* evaluation of PNP hydrogel formulation release kinetics**

(A) Schematic of the *in vitro* release assay of GLP-1 RAs from PNP hydrogels immersed in saline over 2 weeks. *In vitro* release assays were designed to minimize hydrogel erosion by minimizing the surface area-to-volume of the hydrogel.

(B) *In vitro* release profiles showing the percent cumulative release of semaglutide from the 1-10 and 2-10 hydrogel formulations over the course of 2 weeks and their standard deviations ( $n = 3$ ).

(C) *In vitro* release profiles showing the percent cumulative release of liraglutide from the 1-10 and 2-10 hydrogel formulations over the course of 2 weeks and their standard deviations ( $n = 3$ ).

(D) Percent mass of cargo retained in the PNP hydrogel formulations during the release assay after the 2-week release assay show significant difference ( $p < 0.05$ ).

(E) Schematic of the *in vitro* burst release assay of the GLP-1 RAs from PNP hydrogel formulations. Samples ( $n = 3$ ) were directly injected into saline and the supernatant saline was collected after 1 min. Samples were analyzed using either semaglutide- or liraglutide-specific ELISAs. The bar graph shows the percent burst release for each of the hydrogel formulations after 1 min with significant difference ( $p < 0.05$ ).

(F) Schematic illustrating the different release mechanisms of cargo from the PNP hydrogels.

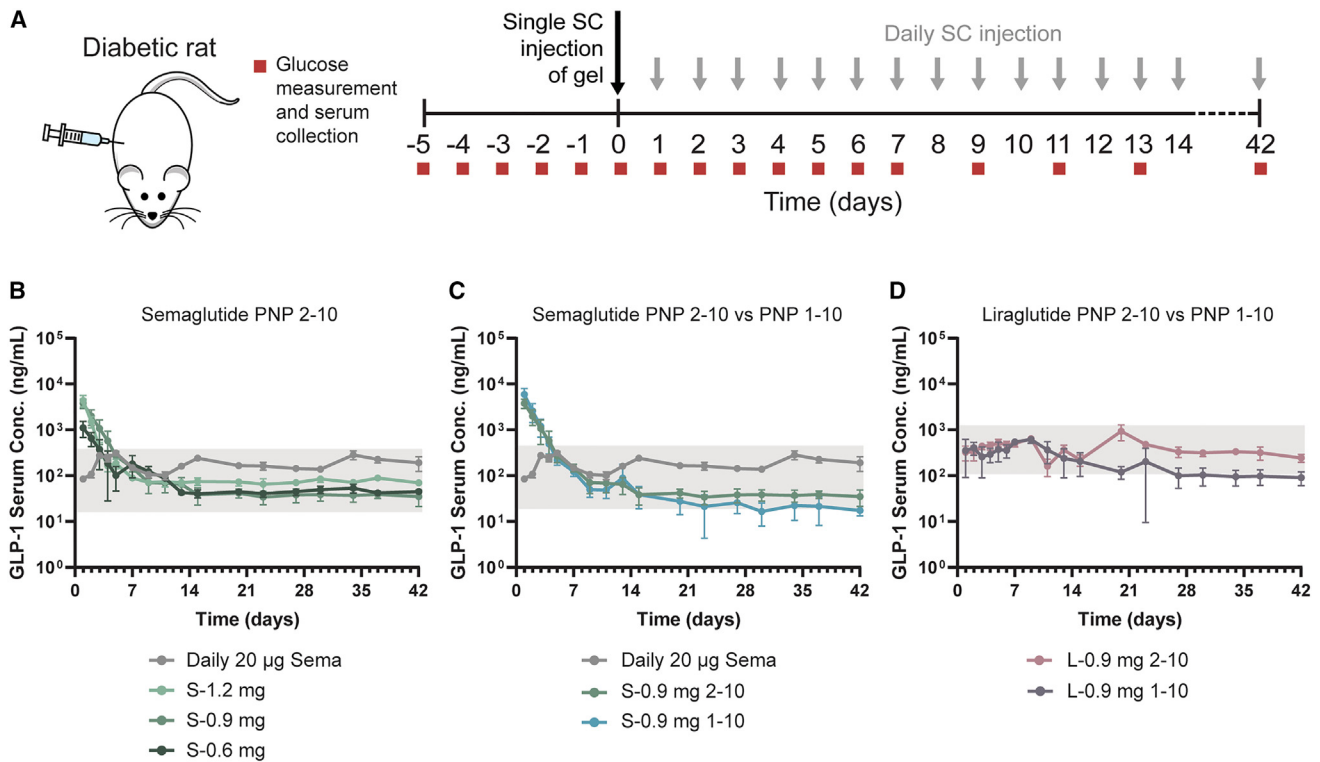


**Figure 4. In vivo evaluation of PNP hydrogel formulation release kinetics in diabetic rats**

Single-dose GLP-1 RA hydrogel treatment prolongs the delivery of semaglutide and liraglutide for 6 weeks compared with a daily 20 µg semaglutide injection. (A) Treatment schedule and timing of blood glucose measurements and serum collection for analysis. Diabetic rats received a single s.c. injection of hydrogel or daily s.c. bolus injections of PBS or daily injections of 20 µg semaglutide.

(B) Pharmacokinetics in diabetic rats and respective standard deviations. Fasted male diabetic rats ( $n = 5-6$ ) received subcutaneous administration of (1) high loading (S-1.2 mg) of semaglutide, (2) medium loading (S-0.9 mg) of semaglutide, or (3) low loading (S-0.6 mg) of semaglutide in the 2-10 formulation.

(C) Comparison of 2-10 vs. 1-10 hydrogel formulation pharmacokinetics and respective standard deviations with the same semaglutide loading (S-0.9 mg).

(D) GLP-1 serum concentration and respective standard deviations for the 2-10 vs. the 1-10 liraglutide hydrogels at a loading of 0.9 mg.

with BG lower than 130 mg/dL or above 200 mg/dL were excluded from the study (Figure 4A). Initially, we validated previously reported pharmacokinetic parameters<sup>23</sup> in diabetic rats (i.e., elimination half-life, volume of distribution, bioavailability, and absorption rate) by conducting a 24-h pharmacokinetics (PK) study following intravenous (i.v.) administration of a 20 µg dose of semaglutide in a saline vehicle (Figure S2). After validating the PK, we conducted an i.v. glucose tolerance test (i.v. GTT) to ensure similar glucose responses when grouping the rats into treatment groups (Method S5). Based on the i.v. GTT, rats with similar glucose tolerance profiles were paired, then these rats were randomized into treatment groups (Figure S3). We then compared the PK following subcutaneous administration of four treatment regimens: (1) repeated daily 20 µg injections of semaglutide in a saline vehicle to mimic current clinical practice,<sup>23</sup> (2) single semaglutide hydrogel formulations, (3) single liraglutide hydrogel formulations, and (4) repeated daily PBS injections as an untreated control ( $n = 5-6$  for each treatment group; Method S3). Semaglutide has a half-life of 7 days in humans at a typical dose of 0.5–1 mg,<sup>56</sup> and PK modeling shows that daily 20 µg dosing in rats recapitulates the current clinical treatment regimen for patients.<sup>32</sup> In contrast, the single-hydrogel treatment groups represent our approach to long-acting GLP-1

RA delivery. For the first 7 days after the start of treatment, and three times a week thereafter, serum was collected for PK analysis and BG was measured (Figure 4A).

The serum concentration of either semaglutide or liraglutide was measured over time following the subcutaneous administration of each treatment by ELISA to assess the PK profile of each hydrogel-based formulation. We hypothesized that our hydrogel formulations would maintain therapeutically relevant concentrations of semaglutide and liraglutide, comparable to daily 20 µg semaglutide administration, for 6 weeks in this rat model. Indeed, all six hydrogel formulations we evaluated in this study effectively maintained relevant concentrations of semaglutide or liraglutide throughout the duration of the 6-week-long study (Figure 4; n.b., the window equivalent to human-relevant serum concentrations for each drug is indicated by the gray box).

One important metric for adverse effects of GLP-1 RA therapies (primarily gastrointestinal discomfort, which is most prevalent when initiating treatment) is  $C_{max}$ , which is the maximum concentration of GLP-1 RA in the serum following treatment. In our studies, daily 20 µg semaglutide administration yielded a  $C_{max}$  of  $280 \pm 60$  ng/mL (observed at day 34), although serum levels were relatively stable over the course of the treatment period with no clear peaks in the PK profile.<sup>56</sup> In contrast, semaglutide-loaded



hydrogels reached very high  $C_{\max}$  values within 1 day of treatment, followed by a continuous decrease in serum concentrations over the course of the first week to a steady state that remained throughout the duration of the study. The  $C_{\max}$  values for each treatment group were  $1,110 \pm 430$  ng/mL (S-0.6 mg 2-10),  $3,800 \pm 900$  ng/mL (S-0.9 mg 2-10), and  $4,400 \pm 1,200$  ng/mL (S-1.2 mg 2-10) (Figure 4B; Table S2). There was a trend toward higher observed  $C_{\max}$  values with increasing dose of semaglutide in these hydrogel formulations, and the highest dose S-1.2 mg 2-10 formulation exhibited significantly higher  $C_{\max}$  values than the S-0.6 mg 2-10 formulation ( $p = 0.0003$ ; Table S2). Similarly, the S-0.9 mg 1-10 formulation exhibited a higher  $C_{\max}$  ( $5,900 \pm 2,100$  ng/mL) compared with the corresponding S-0.9 mg 2-10 formulation ( $3,800 \pm 900$  ng/mL,  $p = 0.09$ ; Table S2). It is important to note that, while the lowest dose hydrogel formulation (S-0.6 mg 2-10) exhibited the lowest  $C_{\max}$  compared with the other hydrogel formulations ( $1,100 \pm 430$  ng/mL), this value was much higher than the  $C_{\max}$  of the daily 20  $\mu$ g semaglutide treatment group ( $280 \pm 60$  ng/mL,  $p = 0.003$ ; Table S2). While the  $C_{\max}$  values observed on the first day for all hydrogel-based semaglutide formulations might be expected to cause nausea and suppressed food intake in rodents, no changes to animal behavior were observed throughout the study.

In contrast to the PK behaviors observed for the semaglutide-based formulations, both liraglutide-based hydrogel formulations quickly established steady-state serum concentrations and did not exhibit any peaks in their PK profiles, indicating a more tolerable profile. The L-0.9 mg 1-10 hydrogel formulation exhibited a  $C_{\max}$  of  $620 \pm 110$  ng/mL (observed on day 9), while the L-0.9 mg 2-10 hydrogel formulation exhibited a  $C_{\max}$  of  $930 \pm 350$  ng/mL (observed on day 20) with relatively steady plasma concentrations throughout the duration of the study (Figure 4D; Table S2). These observations are consistent with the release and retention data described above, whereby the large fraction of “free” semaglutide drug observed within these hydrogel-based formulations would be expected to be released rapidly, thereby contributing to elevated  $C_{\max}$  values at early time points. In contrast, liraglutide was completely retained within the hydrogel depot and would be expected to only be released slowly over time with depot dissolution.

Another important metric for effective therapy is maintenance of appropriate steady-state GLP-1 RA serum concentrations. Each of the six hydrogel-based GLP-1 RA formulations achieved steady-state kinetics throughout the 6-week study, with the semaglutide-loaded 1-10 and 2-10 formulations reaching steady state within 1 week of treatment, while the liraglutide-loaded 1-10 and 2-10 hydrogel formulations reached steady-state within 1 day of treatment (Tables S2 and S3). Consistent with the trends observed for  $C_{\max}$ , a higher semaglutide dose yielded higher  $C_{\text{steady-state}}$  values, whereby the S-1.2 mg 2-10 and S-0.6 mg 2-10 formulations achieved steady-state serum concentrations of  $75 \pm 10$  and  $66 \pm 50$  ng/mL, respectively ( $p = 0.8$ ; Tables S2 and S3).

The hydrogel formulation (i.e., 1-10 vs. 2-10 hydrogels) had less of an impact on steady-state serum concentrations for both semaglutide and liraglutide. Semaglutide-based S-0.9 mg 1-10 and S-0.9 mg 2-10 hydrogel formulations reached similar  $C_{\text{steady-state}}$  values of  $40 \pm 40$  and  $60 \pm 40$  ng/mL, respectively

( $p = 0.3$ ; Tables S2 and S3). Similarly, liraglutide-based L-0.9 mg 1-10 and L-0.9 mg 2-10 hydrogel formulations reached  $C_{\text{steady-state}}$  values of  $270 \pm 190$  and  $410 \pm 200$  ng/mL, respectively ( $p = 0.02$ ; Tables S2 and S3).

### **In vivo pharmacodynamics of hydrogel-based GLP-1 RA formulations**

Next, we examined the ability of the hydrogel-based long-acting GLP-1 RA formulations to reduce average BG after each 6-week treatment regimen. In this study, all GLP-1 RA treatments resulted in a significant reduction in average BG over the course of the study, whereas untreated controls experienced no significant change in average BG (Table S4). While BG dropped more noticeably during the first 2 weeks of the study for the semaglutide hydrogel treatment groups, the reduction was maintained throughout the 6 weeks. The daily dosing of 20  $\mu$ g semaglutide resulted in a  $14\% \pm 4\%$  reduction in average BG over the course of the 6-week study. While a single administration of the S-0.6 mg 2-10 ( $15\% \pm 7\%$  reduction) and S-0.9 mg 2-10 ( $18\% \pm 10\%$  reduction) hydrogel treatments was just as effective at lowering the average BG levels as the daily 20  $\mu$ g semaglutide administrations ( $p = 0.758$  and  $p = 0.586$ , respectively; Figure 5A), a single higher-dose S-1.2 mg 2-10 ( $27\% \pm 2\%$  reduction) hydrogel treatment was significantly more efficacious than the daily 20  $\mu$ g semaglutide dose ( $p = 0.0002$ ; Figure 5A). Moreover, the S-0.9 mg 1-10 hydrogel formulation resulted in a mean reduction in average BG of  $29\% \pm 4\%$ , similar to the S-0.9 mg 2-10 hydrogel formulation, and was also significantly more efficacious than the daily 20  $\mu$ g semaglutide treatment ( $p = 0.0043$ ; Figure 5A). The liraglutide-based hydrogel formulations reduced BG comparable to daily semaglutide administration, with the L-0.9 mg 1-10 and L-0.9 mg 2-10 treatments resulting in mean reductions in average BG of  $20\% \pm 6\%$  ( $p = 0.111$ ) and  $22\% \pm 8\%$  ( $p = 0.0929$ ), respectively.

We also compared the effect of our hydrogel-based GLP-1 RA formulations with that of daily semaglutide treatment on body weight throughout the study (Figure 6). These young growing rats, which increased in body weight over the course of 42 day, exhibited a less pronounced weight gain and a resulting lower body weight at the end of the study when receiving daily semaglutide ( $41\% \pm 10\%$  weight gain) compared with a saline control ( $65\% \pm 13\%$  weight gain) ( $p = 0.0114$ ; Table S4). Similar to our observations above regarding BG, single hydrogel-based treatments resulted in similar weight management compared with daily semaglutide (Figure 6A). For the three semaglutide-based 2-10 hydrogel formulation treatment groups, we observed that the lowest dose S-0.6 mg 2-10 treatments exhibited the greatest increase in weight ( $50\% \pm 11\%$ ;  $p = 0.2066$  with respect to daily semaglutide), while the higher dose S-0.9 mg 2-10 and S-1.2 mg 2-10 treatments exhibited average increases in weight of  $38\% \pm 8\%$  and  $42\% \pm 6\%$  that were similar to that of the daily semaglutide treatment ( $p = 0.6466$  and  $p = 0.8866$  with respect to daily semaglutide). While the S-0.9 mg 2-10 formulation ( $38\% \pm 8\%$ ;  $p = 0.6466$  with respect to daily semaglutide) and the L-0.9 mg 1-10 formulation ( $40 \pm 16\%$ ;  $p = 0.8945$  with respect to daily semaglutide) resulted in the best overall weight management, comparable to daily semaglutide treatment, all hydrogel-based formulations were highly effective at mitigating weight gain in these young, lean growing rats (Figure 6).

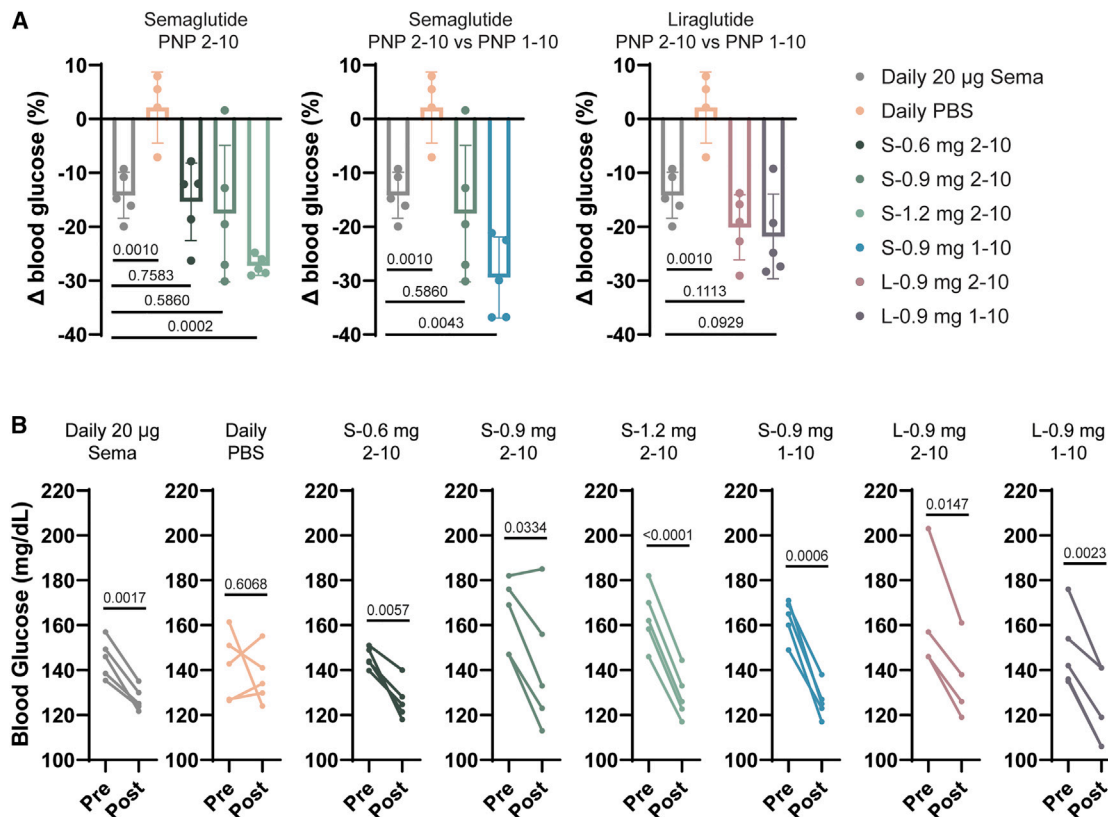


**Figure 5. Effect of PNP hydrogel formulations on blood glucose in diabetic rats**

A single administration of GLP-1 RA hydrogels reduces the BG of type 2-like diabetic male rats over the course of 6 weeks and is similar to or more effective than a treatment regimen consisting of daily semaglutide bolus injections.

(A) Change in BG over 6 weeks following each treatment group regimen ( $n = 5-6$ ).

(B) Individual pre- and post-treatment regimen blood glucose values for individual rats in each treatment group ( $n = 5-6$ ). The  $p$  values were determined using a one-way ANOVA with Dunnett's multiple comparisons test and using an unpaired, two-tailed  $t$  test. [Table S4](#) lists the  $p$  values of each treatment group compared with the PBS control.

### Biocompatibility of hydrogel-based GLP-1 RA therapeutics

Since these hydrogel-based long-acting GLP-1 RA therapeutics are promising drug product candidates, we also sought to assess their biocompatibility. The PNP hydrogels themselves have been shown previously to be highly biocompatible and non-immunogenic in mice, rats, pigs, and sheep in various therapeutic contexts.<sup>33-39,41,44</sup> Here, we sought to conduct histopathological analysis at the endpoint of the rat studies outlined above. A blinded assessment of the histopathology of the liver and kidney of treated animals was conducted 6 weeks after treatment ([Figure S4](#)). The hydrogel-based treatments were shown to be well tolerated, exhibiting no observable differences in liver and kidney compared with both untreated animals and animals receiving daily semaglutide treatment. These results are promising, as they indicate that the hydrogel-based treatments are highly biocompatible.

### Modeling of long-acting liraglutide-hydrogel pharmacokinetics in humans

Based on all of the data described above, the L-0.9 mg 1-10 and 2-10 hydrogel formulations exhibited the most consistent and

favorable PK, reaching steady state after just 1 day and maintaining stable and therapeutically relevant concentrations for the duration of the 42-day study. Yet, beyond evaluating the PK and pharmacodynamics (PD) of hydrogel-based GLP-1 RA therapies, simple PK modeling can be used to predict drug-release kinetics in more clinically relevant large animals and in humans, while also aiding in the design of biomaterial depot technologies.<sup>42</sup> Modeling can inform the optimization of the PNP hydrogel platform for delivery of cargo with similar physicochemical characteristics but different PK characteristics. We have previously reported a simple PK model for depot-based biopharmaceutical formulations following subcutaneous (s.c.) administration, including in PNP hydrogels, based on a two-compartment model that takes into account species-relevant dosing and physiological values for GLP-1 RA PK ([Figure 7A](#)).<sup>57</sup> Here, we used this approach to model the PK for liraglutide in rats following prolonged release from the PNP hydrogel depot and leverage the observed *in vivo* release behaviors to predict the PK of these hydrogel-based liraglutide treatments in humans ([Method S4](#)).

The liraglutide PK for the L-0.9 mg 1-10 was modeled using the half-life of absorption from the s.c. space ( $t_{1/2, \text{s.c.}} \sim 0.16$  h) and

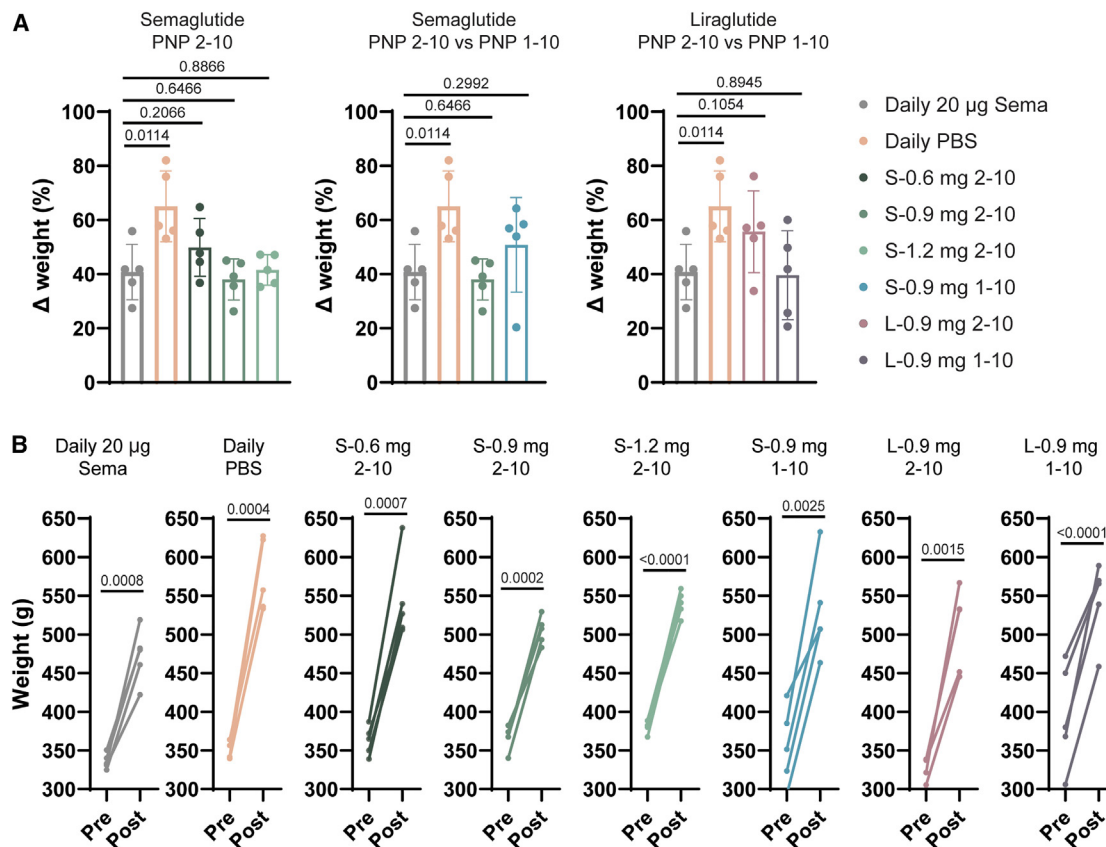


**Figure 6. Effect of PNP hydrogel formulations on weight in diabetic rats**

A single administration of GLP-1 RA hydrogels reduces the overall weight gain in type 2-like diabetic male rats over the course of 6 weeks.

(A) Change in weight over 6 weeks of each treatment group ( $n = 5-6$ ).

(B) Individual pre- and post-treatment weight for individual rats in each treatment group ( $n = 5-6$ ). The  $p$  values were determined using a one-way ANOVA with Dunnett's multiple comparisons test and using an unpaired, two-tailed  $t$  test. Table S4 lists the  $p$  values of each treatment group compared with the PBS control.

the known half-life of elimination from the systemic circulation in rats ( $t_{1/2, \text{serum}} \sim 0.167$  days) (Table S1).<sup>58</sup> This simple two-compartment model sufficiently recapitulates the observed liraglutide PK following release from the s.c. hydrogel depot, suggesting that the model adequately estimates the mass transport processes occurring *in vivo*. This modeling thereby provides insight into the species-independent release characteristics of these materials that enables scaling of the PK to human dosing, assuming full chemical and physical stability of the drug molecule and complete release from the hydrogel depot. For the 500  $\mu$ L injection volume administered in the rats, we observe a rate of liraglutide release of  $\sim 2\%$  per day, which is comparable the erosion rates observed for 100  $\mu$ L administration of PNP-1-10 hydrogels observed previously in mice.<sup>48</sup> These erosion rates correspond to a liraglutide release rate of  $\sim 0.8\%$  per day from a clinically relevant 1.25 mL s.c. injection volume administered in humans. Indeed, the 2.5-fold larger injection volume relevant for human administration will result in a 2.5-fold reduction in the release rate observed in rats (Table S5). Using the expected liraglutide release rate in humans following clinically relevant administration (0.8% per day; 1.25 mL injection volume), relevant human dosing (20 mg), and known human PK parameters for liraglutide ( $t_{1/2, \text{s.c.}}$

$\sim 0.25$  days,  $t_{1/2, \text{serum}} \sim 0.5417$  days),<sup>59</sup> we then modeled the predicted liraglutide PK in humans following hydrogel-based treatments (Figure 7C). This modeling suggests that the 1-10 PNP hydrogel formulation can potentially maintain therapeutically relevant levels of liraglutide in systemic circulation for upward of 120 days from a single administration. From these modeling studies, we observe that a single hydrogel-based treatment has the potential to maintain drug serum concentrations comparable to weekly administrations of semaglutide, one of the leading commercial GLP-1 RA drugs (Figure 7C).

## DISCUSSION

Patient adherence to antihyperglycemic treatment medications is surprisingly low, described for GLP-1 RA to fall between 29% and 54%, resulting in suboptimal T2D management carrying increased risk of stroke, heart and kidney disease, amputation, and blindness.<sup>60</sup> For drugs with short half-lives, poor compliance with prescribed treatment regimens reduces plasma concentrations to unsuitable levels, and multiple doses are often required to return to therapeutic plasma concentrations. Complex and/or frequent administration of treatment is one hurdle

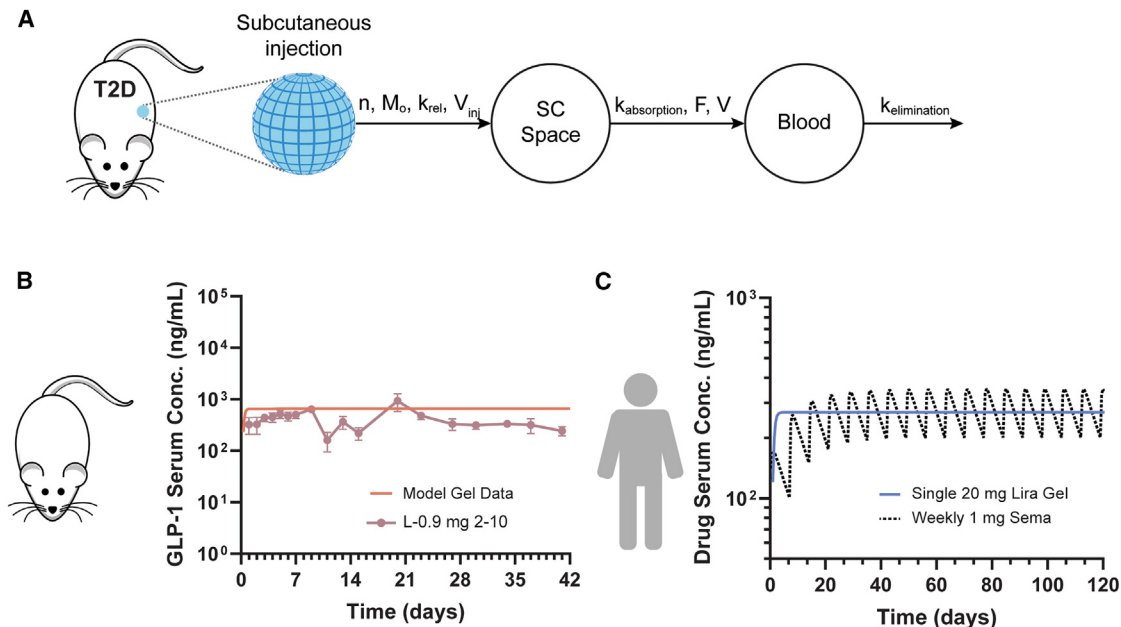


**Figure 7. Pharmacokinetic modeling of hydrogel-based liraglutide formulations in humans**

(A) Scheme showing a two-compartment pharmacokinetic model of drug release from a subcutaneous hydrogel depot. In this model,  $k_{rel}$  and  $n$  are the release parameters of the molecular cargo from the hydrogel depot.

(B) Pharmacokinetics of 0.9 mg liraglutide 1-10 hydrogels in type 2-like diabetic rats following s.c. administration indicate that a single 500  $\mu$ L injection of PNP-1-10 hydrogels can maintain therapeutic concentrations of liraglutide for 6 weeks, while a typical bolus treatment with semaglutide must be administered daily. PK modeling can be used to determine *in vivo* release characteristics for our hydrogel ( $k_{rel}$ ) with known parameters for s.c. absorption and elimination of liraglutide in rats.

(C) Hydrogel release characteristics *in vivo* can be used to estimate PK in humans by using known PK parameters for absorption and elimination and typical drug dosing. Human PK modeling suggests that a single 1.25 mL injection of liraglutide-loaded PNP-1-10 hydrogels can potentially maintain therapeutically relevant concentrations of liraglutide for up to 4 months, matching serum concentrations achieved through weekly injections of commercial semaglutide formulations according to standard dosing regimens.

to adherence. Aligning a GLP-1 RA dosing regimen with the typical schedule of clinical visits has the potential to greatly improve compliance while enabling adjustments to a treatment plan at these visits. A once-every-4-months therapy is likely to be ideal for clinical diabetes management, as this would align with the typical cadence with which patients visit their endocrinologist or personal care provider.

We sought to develop long-acting GLP-1 RA formulations providing months of continuous therapy from a single administration by leveraging an injectable supramolecular hydrogel capable of prolonged delivery of GLP-1 RAs. We hypothesized that one particular class of hydrogel materials, PNP hydrogels, would be particularly well suited to this purpose and would exhibit several important features: (1) facile formulation with important GLP-1 RAs such as semaglutide and liraglutide, (2) patient convenience in the form of straightforward injectability with standard syringes and needles, (3) excellent tolerability by maintaining consistent slow release, and (4) 4 months of continuous therapy per administration. Here, we demonstrated that PNP hydrogel materials enable simple formulation of both semaglutide and liraglutide, which is facilitated by their hydrophobic fatty acid side chains, while maintaining their rheological properties and exhibiting facile injectability. PK modeling of the impact of the difference in typical s.c. administration volumes between rats ( $\sim 0.5$  mL) and humans ( $\sim 1.25$  mL), which directly influences the time frame of hydrogel

erosion and drug release, coupled with the much shorter elimination half-life of GLP-1 RAs in rats (semaglutide  $t_{1/2, serum} \sim 0.29$  days) than in humans (semaglutide  $t_{1/2, serum} \sim 7$  days), indicated that a once-every-4-months therapeutic in humans would exhibit 6 weeks of continuous therapy in rats.

To evaluate the efficacy of our long-acting GLP-1 RA therapeutics, we used an insulin-impaired rat model of T2D. As the half-life of semaglutide is only 0.29 days in rats,<sup>23</sup> the drug must be injected daily to maintain therapeutic concentrations in the systemic circulation. We observed that animals treated daily with 20  $\mu$ g bolus injections of semaglutide for 42 days exhibited a decrease in average BG levels and less pronounced weight gain compared with untreated control rats receiving daily PBS injections. In contrast, we demonstrated that a single administration of PNP hydrogel-based semaglutide or liraglutide drug product candidate maintained therapeutically relevant GLP-1 RA serum concentrations throughout the 42-day study in these T2D rats. Furthermore, a single administration of select hydrogel-based GLP-1 RA formulations, including 2-10 hydrogels comprising a 0.9-mg dose of semaglutide (S-0.9 mg 2-10) and 1-10 hydrogels comprising a 0.9-mg dose of liraglutide (L-0.9 mg 1-10), led to reduced BG levels and improved weight management, in line with daily semaglutide injections over the course of the 42-day study.

While both semaglutide and liraglutide hydrogel-based formulations were shown to improve glucose as well as body weight



control, we found that semaglutide-loaded hydrogel formulations exhibited high  $C_{max}$  values within 1 day of treatment and high drug exposure over the first week of therapy, which is likely to be poorly tolerated in humans. Following the initial exposure, these semaglutide-based hydrogel treatments exhibited a steady-state plateau in serum drug concentrations throughout the duration of the study. In contrast, the liraglutide-loaded hydrogel formulations exhibited no initial peak and reached steady-state serum drug concentrations within 1 day of treatment that persisted throughout the 42-day study. These results suggest that a significant fraction of the semaglutide is released from the hydrogels over the first week, followed by longer-term controlled release. In contrast, all of the liraglutide was found to be entrapped within the hydrogels and released in a more controlled manner, as the hydrogels erode by dissolution over time, providing consistent serum exposure throughout the treatment period. These observations were corroborated by our *in vitro* release studies, which indicated that approximately 50% of entrapped semaglutide is released from the hydrogels within the first week when a plateau was reached, while less than 0.3% of entrapped liraglutide is released under similar conditions.

These results suggest that the semaglutide-loaded hydrogels may contain a significant fraction of “free” cargo that is released diffusively over short time frames from the hydrogels, while the remaining “bound” fraction is released over long time frames as the hydrogels dissolve away. Similarly, liraglutide appears to be entirely “bound” to the hydrogel structure and releases only through hydrogel dissolution and erosion. Previous literature reports have demonstrated that the fatty acid side chain of liraglutide drives the formation of more disorganized heptameric structures at micromolar concentrations,<sup>61</sup> while semaglutide has been reported to form robust dimeric species at similar concentrations.<sup>62,63</sup> In addition, semaglutide’s side-chain linker, which contains two carboxylic acid moieties, is significantly more hydrophilic than that of liraglutide’s, which contains only one carboxylic acid moiety.<sup>23</sup> These physicochemical differences may result in different interactions of the drugs with the hydrophobic interface of the PEG-PLA NPs that constitute the PNP hydrogels. Liraglutide may associate more strongly with the structural motifs within the PNP hydrogels to form such a high “bound” fraction, whereas the robust semaglutide dimers formed at formulation-relevant concentrations constitute the “free” fraction of drug cargo. Importantly for this discussion, semaglutide dimers are sufficiently small ( $R_H < 2$  nm) to be released over relatively short time frames from the PNP hydrogels on account of their comparatively large mesh size ( $\xi \sim 3.5$  nm),<sup>40,62</sup> commensurate with the release behaviors we observed both *in vitro* and *in vivo*.

In addition to demonstrating the PK and PD of these hydrogel-based GLP-1 RA treatments, we have leveraged compartment modeling to demonstrate that a single administration of these drug product candidates can potentially provide upward of 4 months of continuous therapy in humans. Using this approach to PK modeling, which appropriately captured our experimental PK data in rats (Figure 7B; Table S5), enabled us to characterize the release kinetics of the GLP-1 RA drugs from our hydrogel depot *in vivo*. As the administration volume will be much higher for humans ( $\sim 1.25$  mL) than rats ( $\sim 0.5$  mL), modeling shows an extension of the PK to maintain therapeutically relevant serum

concentrations of drug for 120 days, as a larger hydrogel depot will take longer to erode by dissolution (Table S5). Incorporating this type of compartment modeling during the hydrogel material design process is crucial for determining what sort of release behaviors are required to achieve a desired drug PK profile and to ensure that depot technology design is relevant for translation.

This work lays the foundation for translation of advanced hydrogel technologies for the prolonged release of therapeutic peptide-based antidiabetic treatments. We have generated months-long-acting GLP-1 RA drug product candidates forming the basis for a transformational approach to managing diabetes and obesity, which can reduce patient burden by requiring only one injection every 4 months. A single administration of these hydrogel-based treatments provided BG and body weight control comparable to that of 42 administrations of current clinical treatments in a rodent model of T2D. While this research has the potential to affect people with T2D, numerous recent studies suggest that such a product can improve the quality of treatment for people with obesity or T1D as well.<sup>17,64–66</sup> Beyond treatments for diabetes and obesity, this work has the potential to advance the development of long-acting formulations of therapeutic peptides and proteins more broadly.

#### Limitations of the study

As the present study uses a model of diabetes in male Sprague-Dawley rats, it faces limitations related to both the duration of the study and the phenotype of the model. The study was conducted over the course of 6 weeks because of fundamental limitations of the administration volumes in rats. As the duration of release of therapeutic cargo from the injectable hydrogel depot technologies evaluated in this study is dependent on the physical size of the depot, the time frame of the observed PK and PD is limited by the accessible administration volumes. While our PK modeling suggests that larger administration volumes will enable longer-term therapy, further studies must be conducted in larger animals (e.g., swine) to confirm the efficacy of these treatments over longer time frames. Further, we investigated the efficacy of our depot technologies in male rats because of the higher success rate of diabetes induction in male rodents previously reported in the literature. The efficacy of these treatments must be further investigated in the context of both male and female animals in the future.

#### STAR★METHODS

Detailed methods are provided in the online version of this paper and include the following:

- KEY RESOURCES TABLE
- RESOURCE AVAILABILITY
  - Lead contact
  - Materials availability
  - Data and code availability
- EXPERIMENTAL MODEL AND STUDY PARTICIPANT DETAILS
  - Animal model
- METHOD DETAILS
  - Preparations of HPMC-C<sub>12</sub>
  - Preparation of PEG-PLA NPs



- PNP hydrogel preparation
- Rheological characterization of hydrogels
- *In vitro* release
- Animal studies
- Streptozotocin induced diabetes in rats
- 24-hour pharmacokinetics in diabetic rats
- In-vivo pharmacokinetics and pharmacodynamics in diabetic rats
- Biocompatibility
- **QUANTIFICATION AND STATISTICAL ANALYSIS**

### SUPPLEMENTAL INFORMATION

Supplemental information can be found online at <https://doi.org/10.1016/j.xcrm.2023.101292>.

### ACKNOWLEDGMENTS

A.I.D. was supported by a Schmidt Science Fellows Award. C.L.M. was supported by an NSERC Postgraduate Scholarship and Stanford BioX Bowes Graduate Student Fellowship. L.T.N. was supported by a Stanford Graduate Fellowship in Science and Engineering. C.M.K. was supported by the Stanford Bio-X William and Lynda Steere Fellowship. C.K.J. and J.Y. were supported by National Science Foundation Graduate Research Fellowships. We would also like to thank all members of the Appel lab and Novo Nordisk for their useful discussion and advice throughout this project. The authors thank the Stanford Animal Diagnostic Lab and the Veterinary Service Center staff for their technical assistance. Funding for this work is from the National Institute of Diabetes and Digestive and Kidney Diseases (NIDDK) R01 (NIH grant R01DK119254) and a Pilot & Feasibility seed grant from the Stanford Diabetes Research Center (NIH grant P30DK116074).

### AUTHOR CONTRIBUTIONS

Article conceptualization, A.I.D. and E.A.A.; methodology, A.I.D., C.L.M., L.T.N., and E.A.A.; investigation, A.I.D., C.L.M., L.T.N., K.L., A.N.P., I.A.H., S.W.B., C.M.K., C.K.J., J.Y., and E.C.; visualization, A.I.D., C.L.M., and L.T.N.; funding acquisition, E.A.A.; project administration, E.A.A.; supervision, E.A.A.; writing – original draft, A.I.D. and E.A.A.; writing – review & editing, C.L.M., L.T.N., K.L., A.N.P., I.A.H., S.W.B., C.M.K., C.K.J., J.Y., L.H., D.B.S., H.B.A., L.S., and E.A.A.

### DECLARATION OF INTERESTS

A.I.D., C.L.M., L.T.N., and E.A.A. are listed on a patent describing the technology reported in this work. L.H., D.B.S., and H.B.A. declare the following potential competing interest with respect to the research, authorship, and/or publication of this article: the authors are full-time employees and shareholders of Novo Nordisk A/S.

Received: March 16, 2023

Revised: August 2, 2023

Accepted: October 23, 2023

Published: November 21, 2023

### REFERENCES

1. Williams, R., Karuranga, S., Malanda, B., Saeedi, P., Basit, A., Besançon, S., Bommer, C., Esteghamati, A., Ogurtsova, K., Zhang, P., and Colagiuri, S. (2020). Global and regional estimates and projections of diabetes-related health expenditure: Results from the International Diabetes Federation Diabetes Atlas. In *Diabetes Res. Clin. Pract.*, 9th edition, p. 162. <https://doi.org/10.1016/j.diabres.2020.108072>.
2. CDC, Centers for Disease Control and Prevention (2022). National Diabetes Statistics Report Website. <https://www.cdc.gov/diabetes/data/statistics-report/index.html>.
3. Dall, T.M., Yang, W., Gillespie, K., Mocarski, M., Byrne, E., Cintina, I., Beronja, K., Semilla, A.P., Iacobucci, W., and Hogan, P.F. (2019). The Economic Burden of Elevated Blood Glucose Levels in 2017: Diagnosed and Undiagnosed Diabetes, Gestational Diabetes Mellitus, and Prediabetes. *Diabetes Care*, dc181226. <https://doi.org/10.2337/dc18-1226>.
4. DeFronzo, R.A., Ferrannini, E., Groop, L., Henry, R.R., Herman, W.H., Holst, J.J., Hu, F.B., Kahn, C.R., Raz, I., Shulman, G.I., et al. (2015). Type 2 diabetes mellitus. *Nat. Rev. Dis. Prim.* 7, 15019. <https://doi.org/10.1038/nrdp.2015.19>.
5. Olokoba, A.B., Obateru, O.A., and Olokoba, L.B. (2012). Type 2 diabetes mellitus: a review of current trends. *Oman Med. J.* 27, 269–273. <https://doi.org/10.5001/omj.2012.68>.
6. Halban, P.A., Polonsky, K.S., Bowden, D.W., Hawkins, M.A., Ling, C., Mather, K.J., Powers, A.C., Rhodes, C.J., Sussel, L., and Weir, G.C. (2014).  $\beta$ -Cell Failure in Type 2 Diabetes: Postulated Mechanisms and Prospects for Prevention and Treatment. *The Journal of Clinical Endocrinology & Metabolism* 99, 1983–1992. <https://doi.org/10.1210/jc.2014-1425>.
7. Polonsky, W.H., and Henry, R.R. (2016). Poor medication adherence in type 2 diabetes: recognizing the scope of the problem and its key contributors. *Patient Prefer. Adherence* 10, 1299–1307. <https://doi.org/10.2147/ppa.S106821>.
8. Khunti, N., Khunti, N., and Khunti, K. (2019). Adherence to type 2 diabetes management. *Brit J Diab* 19, 99–104. <https://doi.org/10.15277/bjd.2019.223>.
9. Ranganath, L.R. (2008). Incretins: pathophysiological and therapeutic implications of glucose-dependent insulinotropic polypeptide and glucagon-like peptide-1. *J. Clin. Pathol.* 61, 401–409. <https://doi.org/10.1136/jcp.2006.043232>.
10. Nauck, M.A., Quast, D.R., Wefers, J., and Meier, J.J. (2021). GLP-1 receptor agonists in the treatment of type 2 diabetes - state-of-the-art. *Mol. Metabol.* 46, 101102. <https://doi.org/10.1016/j.molmet.2020.101102>.
11. Baggio, L.L., and Drucker, D.J. (2007). Biology of Incretins: GLP-1 and GIP. *Gastroenterology* 132, 2131–2157. <https://doi.org/10.1053/j.gastro.2007.03.054>.
12. Blundell, J., Finlayson, G., Axelsen, M., Flint, A., Gibbons, C., Kvist, T., and Hjerpsted, J.B. (2017). Effects of once-weekly semaglutide on appetite, energy intake, control of eating, food preference and body weight in subjects with obesity. *Diabetes Obes. Metabol.* 19, 1242–1251. <https://doi.org/10.1111/dom.12932>.
13. Gabery, S., Salinas, C.G., Paulsen, S.J., Ahnfelt-Rønne, J., Alanentalo, T., Baquero, A.F., Buckley, S.T., Farkas, E., Fekete, C., Frederiksen, K.S., et al. (2021). Semaglutide lowers body weight in rodents via distributed neural pathways. *JCI Insight* 5. <https://doi.org/10.1172/jci.insight.133429>.
14. Lundgren, J.R., Janus, C., Jensen, S.B.K., Juhl, C.R., Olsen, L.M., Christensen, R.M., Svane, M.S., Bandholm, T., Bojesen-Møller, K.N., Blond, M.B., et al. (2021). Healthy Weight Loss Maintenance with Exercise, Liraglutide, or Both Combined. *N. Engl. J. Med.* 384, 1719–1730. <https://doi.org/10.1056/NEJMoa2028198>.
15. Astrup, A., Rössner, S., Van Gaal, L., Rissanen, A., Niskanen, L., Al Hakim, M., Madsen, J., Rasmussen, M.F., and Lean, M.E.J. (2009). Effects of liraglutide in the treatment of obesity: a randomised, double-blind, placebo-controlled study. *Lancet* 374, 1606–1616. [https://doi.org/10.1016/S0140-6736\(09\)61375-1](https://doi.org/10.1016/S0140-6736(09)61375-1).
16. Pi-Sunyer, X., Astrup, A., Fujioka, K., Greenway, F., Halpern, A., Krempf, M., Lau, D.C.W., le Roux, C.W., Violante Ortiz, R., Jensen, C.B., and Wilding, J.P.H. (2015). A Randomized, Controlled Trial of 3.0 mg of Liraglutide in Weight Management. *N. Engl. J. Med.* 373, 11–22. <https://doi.org/10.1056/NEJMoa1411892>.
17. Iepsen, E.W., Zhang, J., Thomsen, H.S., Hansen, E.L., Hollensted, M., Madsbad, S., Hansen, T., Holst, J.J., Holm, J.-C., and Torekov, S.S.

- (2018). Patients with Obesity Caused by Melanocortin-4 Receptor Mutations Can Be Treated with a Glucagon-like Peptide-1 Receptor Agonist. *Cell Metabol.* 28, 23–32. <https://doi.org/10.1016/j.cmet.2018.05.008>.
18. Wilding, J.P.H., Batterham, R.L., Calanna, S., Davies, M., Van Gaal, L.F., Lingvay, I., McGowan, B.M., Rosenstock, J., Tran, M.T.D., Wadden, T.A., et al. (2021). Once-Weekly Semaglutide in Adults with Overweight or Obesity. *N. Engl. J. Med.* 384, 989–1002. <https://doi.org/10.1056/NEJMoa2032183>.
  19. Jensterle, M., and Janež, A. (2021). Glucagon Like Peptide 1 Receptor Agonists in the Treatment of Obesity. *Horm. Res. Paediatr.* <https://doi.org/10.1159/000521264>.
  20. (2017). Semaglutide and Cardiovascular Outcomes in Patients with Type 2 Diabetes. *N. Engl. J. Med.* 376, 890–892. <https://doi.org/10.1056/NEJMc1615712>.
  21. Marso, S.P., Daniels, G.H., Brown-Frandsen, K., Kristensen, P., Mann, J.F.E., Nauck, M.A., Nissen, S.E., Pocock, S., Poulter, N.R., Ravn, L.S., et al. (2016). Liraglutide and Cardiovascular Outcomes in Type 2 Diabetes. *N. Engl. J. Med.* 375, 311–322. <https://doi.org/10.1056/NEJMoa1603827>.
  22. Gerstein, H.C., Colhoun, H.M., Dagenais, G.R., Diaz, R., Lakshmanan, M., Pais, P., Probstfield, J., Riesenmeyer, J.S., Riddle, M.C., Rydén, L., et al. (2019). Dulaglutide and cardiovascular outcomes in type 2 diabetes (REWIND): a double-blind, randomised placebo-controlled trial. *Lancet* 394, 121–130. [https://doi.org/10.1016/s0140-6736\(19\)31149-3](https://doi.org/10.1016/s0140-6736(19)31149-3).
  23. Knudsen, L.B., and Lau, J. (2019). The Discovery and Development of Liraglutide and Semaglutide. *Front. Endocrinol.* 10, 155. <https://doi.org/10.3389/fendo.2019.00155>.
  24. Weeda, E.R., Muraoka, A.K., Brock, M.D., and Cannon, J.M. (2021). Medication adherence to injectable glucagon-like peptide-1 (GLP-1) receptor agonists dosed once weekly vs once daily in patients with type 2 diabetes: A meta-analysis. *Int. J. Clin. Pract.* 75, e14060. <https://doi.org/10.1111/ijcp.14060>.
  25. Ribel, U., Larsen, M.O., Rolin, B., Carr, R.D., Wilken, M., Sturis, J., Westergaard, L., Deacon, C.F., and Knudsen, L.B. (2002). NN2211: a long-acting glucagon-like peptide-1 derivative with anti-diabetic effects in glucose-intolerant pigs. *Eur. J. Pharmacol.* 451, 217–225. [https://doi.org/10.1016/S0014-2999\(02\)02189-1](https://doi.org/10.1016/S0014-2999(02)02189-1).
  26. Manandhar, B., and Ahn, J.-M. (2015). Glucagon-like Peptide-1 (GLP-1) Analogs: Recent Advances, New Possibilities, and Therapeutic Implications. *J. Med. Chem.* 58, 1020–1037. <https://doi.org/10.1021/jm500810s>.
  27. Association, A.D. (2022). Standards of Medical Care in Diabetes—2022 Abridged for Primary Care Providers. *Clin. Diabetes* 40, 10–38. <https://doi.org/10.2337/cd22-as01>.
  28. Schwendeman, S.P., Shah, R.B., Bailey, B.A., and Schwendeman, A.S. (2014). Injectable controlled release depots for large molecules. *J. Contr. Release* 190, 240–253. <https://doi.org/10.1016/j.jconrel.2014.05.057>.
  29. Sethi, R., and Sanfilippo, N. (2009). Six-month depot formulation of leuprorelin acetate in the treatment of prostate cancer. *Clin. Interv. Aging* 4, 259–267. <https://doi.org/10.2147/cia.s4885>.
  30. Uzoigwe, C., Liang, Y., Whitmire, S., and Paprocki, Y. (2021). Semaglutide Once-Weekly Persistence and Adherence Versus Other GLP-1 RAs in Patients with Type 2 Diabetes in a US Real-World Setting. *Diabetes Ther* 12, 1475–1489. <https://doi.org/10.1007/s13300-021-01053-7>.
  31. Correa, S., Grosskopf, A.K., Lopez Hernandez, H., Chan, D., Yu, A.C., Stapleton, L.M., and Appel, E.A. (2021). Translational Applications of Hydrogels. *Chem. Rev.* 121, 11385–11457. <https://doi.org/10.1021/acs.chemrev.0c01177>.
  32. Appel, E.A., Tibbitt, M.W., Webber, M.J., Mattix, B.A., Veisoh, O., and Langer, R. (2015). Self-assembled hydrogels utilizing polymer–nanoparticle interactions. *Nat. Commun.* 6, 6295. <https://doi.org/10.1038/ncomms7295>.
  33. Grosskopf, A.K., Roth, G.A., Smith, A.A.A., Gale, E.C., Hernandez, H.L., and Appel, E.A. (2020). Injectable supramolecular polymer–nanoparticle hydrogels enhance human mesenchymal stem cell delivery. *Bioengineering & Translational Medicine* 5, e10147. <https://doi.org/10.1002/btm2.10147>.
  34. Stapleton, L.M., Steele, A.N., Wang, H., Lopez Hernandez, H., Yu, A.C., Paulsen, M.J., Smith, A.A.A., Roth, G.A., Thakore, A.D., Lucian, H.J., et al. (2019). Use of a supramolecular polymeric hydrogel as an effective post-operative pericardial adhesion barrier. *Nat. Biomed. Eng.* 3, 611–620. <https://doi.org/10.1038/s41551-019-0442-z>.
  35. Steele, A.N., Stapleton, L.M., Farry, J.M., Lucian, H.J., Paulsen, M.J., Eskandari, A., Hironaka, C.E., Thakore, A.D., Wang, H., Yu, A.C., et al. (2019). A Biocompatible Therapeutic Catheter-Deliverable Hydrogel for In Situ Tissue Engineering. *Adv. Healthcare Mater.* 8, 1801147. <https://doi.org/10.1002/adhm.201801147>.
  36. Yu, A.C., Lian, H., Kong, X., Lopez Hernandez, H., Qin, J., and Appel, E.A. (2021). Physical networks from entropy-driven non-covalent interactions. *Nat. Commun.* 12, 746. <https://doi.org/10.1038/s41467-021-21024-7>.
  37. Meis, C.M., Grosskopf, A.K., Correa, S., and Appel, E.A. (2021). Injectable Supramolecular Polymer–Nanoparticle Hydrogels for Cell and Drug Delivery Applications. *JoVE* e62234. <https://doi.org/10.3791/62234>.
  38. Liong, C.S., Smith, A.A.A., Mann, J.L., Roth, G.A., Gale, E.C., Maikawa, C.L., Ou, B.S., and Appel, E.A. (2021). Enhanced Humoral Immune Response by High Density TLR Agonist Presentation on Hyperbranched Polymers. *Advanced Therapeutics* 2021, 2000081. <https://doi.org/10.1002/adtp.202000081>.
  39. Stapleton, L.M., Lucian, H.J., Grosskopf, A.K., Smith, A.A.A., Thetherow, K.P., Woo, Y.J., and Appel, E.A. (2021). Dynamic Hydrogels for Prevention of Post-Operative Peritoneal Adhesions. *Advanced Therapeutics* 2000242. <https://doi.org/10.1002/adtp.202000242>.
  40. Roth, G.A., Gale, E.C., Alcántara-Hernández, M., Luo, W., Axpe, E., Verma, R., Yin, Q., Yu, A.C., Lopez Hernandez, H., Maikawa, C.L., et al. (2020). Injectable Hydrogels for Sustained Codelivery of Subunit Vaccines Enhance Humoral Immunity. *ACS Cent. Sci.* 6, 1800–1812. <https://doi.org/10.1021/acscentsci.0c00732>.
  41. Roth, G.A., Saouaf, O.M., Smith, A.A.A., Gale, E.C., Hernández, M.A., Idayaga, J., and Appel, E.A. (2021). Prolonged Codelivery of Hemagglutinin and a TLR7/8 Agonist in a Supramolecular Polymer–Nanoparticle Hydrogel Enhances Potency and Breadth of Influenza Vaccination. *ACS Biomater. Sci. Eng.* <https://doi.org/10.1021/acsbio-materials.0c01496>.
  42. Kasse, C.M., Yu, A.C., Powell, A.E., Roth, G.A., Liong, C.S., Jons, C.K., Buahin, A., Maikawa, C.L., Youssef, S., Gianville, J.E., and Appel, E.A. (2022). Subcutaneous delivery of an antibody against SARS-CoV-2 from a supramolecular hydrogel depot. Preprint at bioRxiv. <https://doi.org/10.1101/2022.05.24.493347>.
  43. Grosskopf, A.K., Labanieh, L., Klysz, D.D., Roth, G.A., Xu, P., Adebowale, O., Gale, E.C., Jons, C.K., Klich, J.H., Yan, J., et al. (2022). Delivery of CAR-T cells in a transient injectable stimulatory hydrogel niche improves treatment of solid tumors. *Sci. Adv.* 8, eabn8264. <https://doi.org/10.1126/sciadv.abn8264>.
  44. Lopez Hernandez, H., Grosskopf, A.K., Stapleton, L.M., Agmon, G., and Appel, E.A. (2019). Non-Newtonian Polymer–Nanoparticle Hydrogels Enhance Cell Viability during Injection. *Macromol. Biosci.* 19, 1800275. <https://doi.org/10.1002/mabi.201800275>.
  45. Lopez Hernandez, H., Souza, J.W., and Appel, E.A. (2021). A Quantitative Description for Designing the Extrudability of Shear-Thinning Physical Hydrogels. *Macromol. Biosci.* 21, 2000295. <https://doi.org/10.1002/mabi.202000295>.
  46. Spector, A.A. (1975). Fatty acid binding to plasma albumin. *J. Lipid Res.* 16, 165–179.
  47. Kontermann, R.E. (2011). Strategies for extended serum half-life of protein therapeutics. *Curr. Opin. Biotechnol.* 22, 868–876. <https://doi.org/10.1016/j.copbio.2011.06.012>.
  48. Jons, C.K., Grosskopf, A.K., Baillet, J., Yan, J., Klich, J.H., Saouaf, O.M., and Appel, E.A. (2022). Yield-Stress and Creep Control Depot Formation and

- Persistence of Injectable Hydrogels Following Subcutaneous Administration. *Adv. Funct. Mater.* 32, 2203402. <https://doi.org/10.1002/adfm.202203402>.
49. Nair, A.B., and Jacob, S. (2016). A simple practice guide for dose conversion between animals and human. *J. Basic Clin. Pharm.* 7, 27–31. <https://doi.org/10.4103/0976-0105.177703>.
  50. Jensen, L., Helleberg, H., Roffel, A., van Lier, J.J., Bjørnsdottir, I., Pedersen, P.J., Rowe, E., Derving Karsbøl, J., and Pedersen, M.L. (2017). Absorption, metabolism and excretion of the GLP-1 analogue semaglutide in humans and nonclinical species. *Eur. J. Pharmaceut. Sci.* 104, 31–41. <https://doi.org/10.1016/j.ejps.2017.03.020>.
  51. Appel, E.A., Forster, R.A., Rowland, M.J., and Scherman, O.A. (2014). The control of cargo release from physically crosslinked hydrogels by crosslink dynamics. *Biomaterials* 35, 9897–9903. <https://doi.org/10.1016/j.biomaterials.2014.08.001>.
  52. Szkudelski, T. (2012). Streptozotocin–nicotinamide-induced diabetes in the rat. Characteristics of the experimental model. *Exp. Biol. Med.* 237, 481–490. <https://doi.org/10.1258/ebm.2012.011372>.
  53. Masiello, P., Broca, C., Gross, R., Roye, M., Manteghetti, M., Hillaire-Buys, D., Novelli, M., and Ribes, G. (1998). Experimental NIDDM: development of a new model in adult rats administered streptozotocin and nicotinamide. *Diabetes* 47, 224–229. <https://doi.org/10.2337/diab.47.2.224>.
  54. Chen, T., Kagan, L., and Mager, D.E. (2013). Population pharmacodynamic modeling of exenatide after 2-week treatment in STZ/NA diabetic rats. *J Pharm Sci* 102, 3844–3851. <https://doi.org/10.1002/jps.23682>.
  55. Wu, K.K., and Huan, Y. (2008). Streptozotocin-induced diabetic models in mice and rats. *Curr. Protoc. Pharmacol.* Chapter 5, Unit 5.47. <https://doi.org/10.1002/0471141755.ph0547s40>.
  56. Hall, S., Isaacs, D., and Clements, J.N. (2018). Pharmacokinetics and Clinical Implications of Semaglutide: A New Glucagon-Like Peptide (GLP)-1 Receptor Agonist. *Clin. Pharmacokinet.* 57, 1529–1538. <https://doi.org/10.1007/s40262-018-0668-z>.
  57. Gibaldi, M.P.D. (1982). *Pharmacokinetics*, 2nd ed. (Marcel Dekker).
  58. Sturis, J., Gotfredsen, C.F., Rømer, J., Rolin, B., Ribel, U., Brand, C.L., Wilken, M., Wassermann, K., Deacon, C.F., Carr, R.D., and Knudsen, L.B. (2003). GLP-1 derivative liraglutide in rats with beta-cell deficiencies: influence of metabolic state on beta-cell mass dynamics. *Br. J. Pharmacol.* 140, 123–132. <https://doi.org/10.1038/sj.bjp.0705397>.
  59. Jackson, S.H., Martin, T.S., Jones, J.D., Seal, D., and Emanuel, F. (2010). Liraglutide (victoza): the first once-daily incretin mimetic injection for type-2 diabetes. *P t* 35, 498–529.
  60. Giorgino, F., Penforinis, A., Pechtner, V., Gentilella, R., and Corcos, A. (2018). Adherence to antihyperglycemic medications and glucagon-like peptide 1-receptor agonists in type 2 diabetes: clinical consequences and strategies for improvement. *Patient Prefer. Adherence* 12, 707–719. <https://doi.org/10.2147/PPA.S151736>.
  61. Steensgaard, D., Thomsen, J.K., Olsen, H.B., and Knudsen, L.B. (2008). The molecular basis for the delayed absorption of the once-daily human GLP-1 analogue, Liraglutide. *Diabetes* 57, A164.
  62. Venanzi, M., Savioli, M., Cimino, R., Gatto, E., Palleschi, A., Ripani, G., Cicero, D., Placidi, E., Orvieto, F., and Bianchi, E. (2020). A spectroscopic and molecular dynamics study on the aggregation process of a long-acting lipidated therapeutic peptide: the case of semaglutide. *Soft Matter* 16, 10122–10131. <https://doi.org/10.1039/D0SM01011A>.
  63. Lau, J., Bloch, P., Schäffer, L., Pettersson, I., Spetzler, J., Kofoed, J., Madson, K., Knudsen, L.B., McGuire, J., Steensgaard, D.B., et al. (2015). Discovery of the Once-Weekly Glucagon-Like Peptide-1 (GLP-1) Analogue Semaglutide. *J. Med. Chem.* 58, 7370–7380. <https://doi.org/10.1021/acs.jmedchem.5b00726>.
  64. Rosenstock, J., Bajaj, H.S., Janež, A., Silver, R., Begtrup, K., Hansen, M.V., Jia, T., and Goldenberg, R. (2020). Once-Weekly Insulin for Type 2 Diabetes without Previous Insulin Treatment. *N. Engl. J. Med.* 383, 2107–2116. <https://doi.org/10.1056/NEJMoa2022474>.
  65. Sofrà, D. (2019). Impact of adding semaglutide in a person with type 1 diabetes: A case report. *Diabetes Updates* 5. <https://doi.org/10.15761/DU.1000128>.
  66. Goyal, I., Sattar, A., Johnson, M., and Dandona, P. (2020). Adjunct therapies in treatment of type 1 diabetes. *J. Diabetes* 12, 742–753. <https://doi.org/10.1111/1753-0407.13078>.
  67. Meis, C.M., Salzman, E.E., Maikawa, C.L., Smith, A.A.A., Mann, J.L., Grosskopf, A.K., and Appel, E.A. (2021). Self-Assembled, Dilution-Responsive Hydrogels for Enhanced Thermal Stability of Insulin Biopharmaceuticals. *ACS Biomater. Sci. Eng.* 7, 4221–4229. <https://doi.org/10.1021/acsbomaterials.0c01306>.
  68. Galderisi, A., Schlissel, E., and Cengiz, E. (2017). Keeping Up with the Diabetes Technology: 2016 Endocrine Society Guidelines of Insulin Pump Therapy and Continuous Glucose Monitor Management of Diabetes. *Curr. Diabetes Rep.* 17, 111. <https://doi.org/10.1007/s11892-017-0944-6>.

## STAR★METHODS

### KEY RESOURCES TABLE

REAGENT or RESOURCE	SOURCE	IDENTIFIER
<b>Chemicals, peptides, and recombinant proteins</b>		
Hydroxypropyl methyl cellulose	Sigma-Aldrich	Cat# 423203
N,N-diisopropylethylamine (Hunig's base)	Sigma-Aldrich	Cat# D125806
Hexanes	Sigma-Aldrich	Cat# 208752
diethyl ether	Sigma-Aldrich	Cat# 296082
N-methyl-2-pyrrolidone (NMP)	Sigma-Aldrich	Cat# 328634
dichloromethane (DCM)	Sigma-Aldrich	Cat# 270997
3,6-Dimethyl-1,4-dioxane-2,5-dione (lactide, LA)	Sigma-Aldrich	Cat# 303143
1,8-Diazabicyclo[5.4.0]undec-7-ene (DBU)	Sigma-Aldrich	Cat# 139009
1-dodecyl isocyanate	Sigma-Aldrich	Cat# 389064
Poly(ethylene glycol) methyl ether (5 kDa)	Sigma-Aldrich	Cat# 81323
Semaglutide	NovoNordisk	N/A
Liraglutide	NovoNordisk	N/A
<b>Critical commercial assays</b>		
Semaglutide, ELISA Kit, high sensitivity	BMA Biomedicals	Cat# S-1530
Liraglutide, ELISA Kit, high sensitivity	BMA Biomedicals	Cat# S-1502
<b>Experimental models: Organisms/strains</b>		
Sprague Dawley Male Rats (albino)	Charles River	Strain# 001
<b>Software and algorithms</b>		
Prism version 9.5.1	Graphpad	<a href="https://www.graphpad.com/features">https://www.graphpad.com/features</a>
Adobe Illustrator 2023	Adobe	<a href="https://www.adobe.com/products/illustrator.html">https://www.adobe.com/products/illustrator.html</a>
JMP Pro16	JMP	<a href="https://www.jmp.com/en_us/events/mastering/topics/new-in-jmp16-and-jmp-pro16.html">https://www.jmp.com/en_us/events/mastering/topics/new-in-jmp16-and-jmp-pro16.html</a>

### RESOURCE AVAILABILITY

#### Lead contact

Further information and requests for resources and reagents should be directed to and will be fulfilled by the lead contact, Prof. Eric Appel ([eappel@stanford.edu](mailto:eappel@stanford.edu)).

#### Materials availability

Materials generated in this study are available upon reasonable request from the [lead contact](#) with a complete Materials Transfer Agreement through Stanford University's Industrial Contracts Office.

#### Data and code availability

- Data reported in this paper and associated documentation is available upon reasonable request from the [lead contact](#) under agreements providing for a commitment to using the data only for research purposes, a commitment to securing the data using appropriate computer technology, destruction of the data after analyses are completed, restrictions of redistribution of the data to third parties, proper acknowledgement of the data resource, and restrictions ensuring that information provided will not be used for commercial purposes.
- This paper does not report code.
- Any additional information required to reanalyze the data reported in this work paper is available upon reasonable request from the [lead contact](#).

## EXPERIMENTAL MODEL AND STUDY PARTICIPANT DETAILS

### Animal model

Male, albino Sprague Dawley rats (Charles River) were used for experiments and were purchased at 7 weeks old at the start of the study. The Sprague Dawley rats provide well-established and reproducible models of streptozotocin-induced type-2 like insulin-deficient diabetes. Rats are a better model than mice because the larger blood volume allows for more frequent blood glucose assessment and pharmacokinetic analysis of GLP-1 RAs. Animal studies were performed in accordance with the guidelines for the care and use of laboratory animals; all protocols were approved by the Stanford Institutional Animal Care and Use Committee (Protocol #32873). Rats were doubly housed in Stanford's animal facilities in specific pathogen-free conditions in accordance with the Institutional Animal Care and Use Committee guidelines. Male rats were used in this study owing to their higher proclivity for developing diabetes according to standard diabetes induction protocols. Female rats have been reported to be less responsive to classic diabetes protocols, which is a limitation of this work.

## METHOD DETAILS

### Preparations of HPMC-C<sub>12</sub>

Dodecyl-modified (hydroxypropyl)methyl cellulose (HPMC-C<sub>12</sub>) was prepared according to previously reported procedures.<sup>67</sup> HPMC (1.0 g) was dissolved in NMP (40 mL) by stirring at 80 °C for 1 h. Once the solution reached room temperature (RT), 1-dodecylisocyanate (105 mg, 0.5 mmol) and N,N-diisopropylethylamine (catalyst, ~3 drops) were dissolved in NMP (5.0 mL). This solution was added dropwise to the reaction mixture, which was then stirred at RT for 16 h. This solution was then precipitated from acetone, decanted, redissolved in water (~2 wt%), and placed in a dialysis tube for dialysis for 3–4 days. The polymer was lyophilized and reconstituted to a 60 mg mL<sup>-1</sup> solution with sterile PBS.

### Preparation of PEG-PLA NPs

PEG-PLA was prepared as previously reported.<sup>67</sup> Monomethoxy-PEG (5 kDa; 0.25 g, 4.1 mmol) and DBU (15 μL, 0.1 mmol; 1.4 mol% relative to LA) were dissolved in anhydrous dichloromethane (1.0 mL). LA (1.0 g, 6.9 mmol) was dissolved in anhydrous DCM (3.0 mL) with mild heating. The LA solution was added rapidly to the PEG/DBU solution and was allowed to stir for 10 min. The reaction mixture was quenched and precipitated by a 1:1 hexane and ethyl ether solution. The synthesized PEG-PLA was collected and dried under vacuum. Hydrogel permeation chromatography (GPC) was used to verify that the molecular weight and dispersity of polymers meet our quality control (QC) parameters. NPs were prepared as previously reported<sup>67</sup>. A 1 mL solution of PEG-PLA in DMSO (50 mg mL<sup>-1</sup>) was added dropwise to 10 mL of water at RT under a high stir rate (600 rpm). NPs were purified by centrifugation over a filter (molecular weight cutoff of 10 kDa; Millipore Amicon Ultra-15) followed by resuspension in PBS to a final concentration of 200 mg mL<sup>-1</sup>. NPs were characterized by dynamic light scattering (DLS) to find the NP diameter, 37 ± 4 nm.

### PNP hydrogel preparation

Hydrogel formulations contained either 2 wt% HPMC-C<sub>12</sub> and 10 wt% PEG-PLA NPs in PBS, or 1 wt% HPMC-C<sub>12</sub> and 10 wt% PEG-PLA NPs in PBS. These hydrogels were made by mixing a 2:3:1 weight ratio of 6 wt% HPMC-C<sub>12</sub> polymer solution, 20 wt% NP solution, and PBS containing GLP-1 RAs. The NP and aqueous components were loaded into one syringe, the HPMC-C<sub>12</sub> was loaded into a second syringe and components were mixed using an elbow connector. After mixing, the elbow was replaced with a 21-gauge needle for injection.

### Rheological characterization of hydrogels

Rheological testing was performed at 25 °C using a 20-mm-diameter serrated parallel plate at a 600 μm gap on a stress-controlled TA Instruments DHR-2 rheometer. All experiments were performed at 25 °C. Frequency sweeps were performed from 0.1 to 100 rad s<sup>-1</sup> with a constant oscillation strain within the linear viscoelastic regime (1%). Amplitude sweeps were performed at a constant angular frequency of 10 rad s<sup>-1</sup> from 0.01% to 10000% strain with a gap height of 500 μm. Flow sweeps were performed from low to high stress with steady-state sensing. Steady shear experiments were performed by alternating between a low shear rate (0.1 s<sup>-1</sup>) and high shear rate (10 s<sup>-1</sup>) for 60 s each for three full cycles. Shear rate sweep experiments were performed from 10 to 0.001 s<sup>-1</sup>. Stress controlled yield stress measurements (stress sweeps) were performed from low to high stress with steady-state sensing and 10 points per decade.

### In vitro release

100 μL of each hydrogel formulation was loaded into four-inch capillaries and 400 μL of PBS medium was added slowly on top. The surrounding PBS was removed for analysis after 1, 3, 6, 12, 24, and 48 hours and at one week and two weeks after injection into the capillary, and fresh PBS was replaced after each aliquot removal. Semaglutide and liraglutide were quantified by ELISA to determine release kinetics over time.



### Animal studies

Animal studies were performed with the approval of the Stanford Administrative Panel on Laboratory Animal Care (APLAC-32873) in accordance with NIH guidelines.

#### Streptozotocin induced diabetes in rats

Male Sprague Dawley rats (Charles River) were used for experiments. Animal studies were performed in accordance with the guidelines for the care and use of laboratory animals; all protocols were approved by the Stanford Institutional Animal Care and Use Committee (Protocol #32873). Briefly, male Sprague Dawley rats 160–230 g (8–10 weeks) were weighed and fasted in the morning 6–8 h prior to treatment with nicotinamide (NA) and streptozotocin (STZ). NA was dissolved in 1X PBS and administered intraperitoneally at 110 mg/kg. STZ was diluted to 10 mg mL<sup>-1</sup> in the sodium citrate buffer immediately before injection. STZ solution was injected intraperitoneally at 65 mg kg<sup>-1</sup> into each rat. Rats were provided with water containing 10% sucrose for 24 h after injection with STZ. Rat BG levels were tested for hyperglycemia daily after the STZ treatment via tail vein blood collection using a hand-held Bayer Contour Next glucose monitor (Bayer). Rats were considered diabetic when at least three out of five fasting BG measurements, taken over the course of five days, fell between 130–200 mg/dL.

#### 24-hour pharmacokinetics in diabetic rats

A 24-hour PK study was conducted to validate previously reported pharmacokinetic parameters (i.e., elimination half-life, volume of distribution, bioavailability, and absorption rate) of semaglutide in rats, whereby semaglutide (20 μg) was administered via bolus injection using two routes of administration, including subcutaneous (SC) and intravenous (IV). Six rats received each treatment and blood samples were collected from the tail vein every 30 minutes after treatment for eight hours, and then again at 18 hours and 24 hours.

#### In-vivo pharmacokinetics and pharmacodynamics in diabetic rats

For each of the treatment groups (n = 5–6), baseline blood was collected from the tail vein at day zero and daily blood glucose measurements were taken from the tail vein using a handheld blood glucose monitor (Bayer Contour Next) for 42 days following treatment.<sup>68</sup> Blood glucose was measured, immediately followed by blood samples collected from the tail vein, every day for the first seven days of the study to measure serum semaglutide concentrations using ELISA, and two times a week, thereafter. Materials for these assays were made available to us by Novo Nordisk through their compound sharing program. Plasma GLP-1 RA concentrations were measured by ELISA at each time-point and total bioavailability of semaglutide was determined at the end-point of the study. An IV glucose tolerance test<sup>54</sup> was used to group rats according to the glucose tolerance before treatment (at day -1).

#### Biocompatibility

At the end of the 6-week experiment, the rats were euthanized using carbon dioxide and tissues (kidneys and liver) were collected for histology. The harvested tissue was fixed and transverse sections of the left lateral lobe and right medial lobe of the liver as well as longitudinal sections of the kidney were taken for histological analysis. Haematoxylin and eosin staining were performed by Histotec Laboratory.

### QUANTIFICATION AND STATISTICAL ANALYSIS

All results are expressed as a mean ± standard deviation unless specified otherwise. For in-vivo experiments, Mead's Resource Equation was used to identify a sample size above that additional subjects will have little impact on power. Comparison between groups was conducted with the Tukey HSD test in JMP. A one-way analysis of variance (ANOVA) or a t-test was also used to compare groups. A difference of p < 0.05 was considered statistically significant.